Title

Sympathetic Remodeling and Cardiac Electrophysiology in the Rabbit Heart

Author

Guevara, Amanda Marie

Publication Date

2023

Peer reviewed|Thesis/dissertation

Sympathetic Remodeling and Cardiac Electrophysiology in the Rabbit Heart

By

AMANDA GUEVARA
DISSERTATION

Submitted in partial satisfaction of the requirements for the degree for

DOCTOR OF PHILOSOPHY

in

Molecular, Cellular, and Integrative Physiology

in the

OFFICE OF GRADUATE STUDIES

of the

UNIVERSITY OF CALIFORNIA

DAVIS

Approved:

_____
Crystal M. Ripplinger, Chair

_____
Madeline Nieves-Cintron

_____
Chao-Yin Chen

Committee in Charge

2023

Table of Contents

List of Figures

Acknowledgements

I would like to thank Dr. Crystal Ripplinger, my PhD advisor and chair of my dissertation committee for giving me the opportunity to be part of the Ripplinger lab where we conduct pretty cool research and have fun while doing it! Thank you for your encouragement, patience, and feedback. I am extremely lucky to have had such a supportive mentor throughout my doctoral program. I would also like to thank my dissertation committee members Dr. Madeline Nieves-Cintron and Dr. Chao-Yin Chen. Thank you for your time, feedback, and encouragement throughout my time at UC Davis.

Thank you to my family for all the love and support you have given me my entire life. Thank you to my mother Michelle Guevara for being my #1 fan in everything that I do. Thank you especially to my father Dr. Amado Guevara, I miss you everyday. Thank you to my martial arts and gym family for being supportive and keeping me sane during college and graduate school. Special thank you to my martial arts instructor and "second" mother Linda Pulido. I am forever grateful for everything you have taught me in martial arts and in life. Thank you to my ride or dies Patty and Sadaf for always being there.

Dr. Samantha Francis Stuart, Lena Ngo, Dr. Srinu Tapa, and Dr. Zhen Wang - thank you for your help on the nicotine project. HUGE thank yous to: Dr. Charlotte Smith, Dr. Jessica Caldwell, Eric I-Ju Lee and Lilian Mott. The entire nicotine project would never have been completed if I didn't have all of your help or encouragement. It was alot of work (but we had fun ☺) and I am extremely proud of the work we have produced and I cannot wait for it to be shared. Special thank you to Team Camper and Team Disaster – thanks for the disasters (the haha ones, not the fml ones), the laughs, and for just being my friends. Thank you to Dr. Lianguo Wang for fixing said disasters and for all of the knowledge you have shared. I am so very grateful for all of you and words cannot express my gratitude.

Lastly, a special thank you to my ride or die, coolest co-pilot, best gym partner, and favorite couch surfer; Cooper. From joining me in a HIIT class, to paddleboarding on the lake, or going topless in the Jeep, you have been a constant source of love, fun, and cuddles. Cooper you have made my entire PhD career for me. Thank you. Oh and yes thank you to you too Harmony and Lilly (my cats) ☺.

This is cooper in case you were wondering

Sympathetic Remodeling and Cardiac Electrophysiology in the Rabbit Heart

Abstract

This dissertation focuses on the impact of sympathetic remodeling and its effects on cardiac electrophysiology. We were able to use a fully innervated rabbit heart preparation and whole heart dual-optical mapping to directly stimulate sympathetic nerve fibers to investigate the electrophysiological changes that occur in response to nerve stimulation. By using both direct sympathetic nerve stimulation and ß-adrenergic agonists we were able to characterize the effect myocardial infarction and chronic nicotine exposure have on sympathetic remodeling and hyperactivity. We evaluated the role that chondroitin sulfate proteoglycans (CSPG) have in sympathetic nerve *hypo*-innervation after myocardial infarction in the rabbit heart and the resulting electrophysiological consequences. We found that CSPGs are present in the *hypo*-innervated infarct region and that *hypo*-innervation results in changes in Ca^{2+} handling and alterations in cardiac electrophysiology; these results confirm previous rodent work. Additionally, we characterized the effect chronic nicotine has on Ca^{2+} mishandling, electrophysiological changes, and arrhythmia susceptibility. We found that 4 weeks of chronic nicotine exposure results in sympathetic *hypo*-innervation of the myocardium, diminished adrenergic responsiveness, and potentially detrimental sympathetic and electrophysiological remodeling. This dissertation provides a comprehensive perspective on how the effects of sympathetic remodeling and hyperactivity on cardiac electrophysiology in the rabbit heart.

Chapter 1: Introduction

The Autonomic Nervous System

General Anatomy and Physiology:

The nervous system is composed of the central and peripheral nervous systems. The autonomic nervous system is a subdivision of the nervous system and is composed of portions from both the central and peripheral nervous systems. The primary function of the autonomic nervous system is to maintain homeostasis by coordinating adaptive responses to stress (Jamali, Waqar, and Gerson 2017; Gibbons 2019). One example of this role can be seen in the regulation of involuntary functions such as blood pressure, heart rate, and respiration. The autonomic nervous system is composed of three major divisions: the sympathetic nervous system, parasympathetic nervous system, and enteric nervous system. The enteric nervous system has nerves and nerve cells located within the wall of the gastrointestinal tract and is crucial in regulating gut motility, secretion of digestive enzymes, and blood flow to digestive organs. For the scope of this dissertation, the enteric nervous system will not be discussed. Both the sympathetic and parasympathetic nervous systems are considered a "two neuron pathway" such that the preganglionic neurons have cell bodies located within the central nervous system that release acetylcholine (ACh), which binds nicotinic acetylcholine receptors (nAChR) located on postganglionic neurons in the peripheral nervous system. These postganglionic neurons then have axons that extend out to target tissues such as glands, smooth muscle, or cardiac muscle. However, the sympathetic and parasympathetic nervous systems differ in their organization of

neurons, physiological responses, the type of neurotransmitters that are released, and its associated receptor.

The sympathetic nervous system is generally referred to as the “fight or flight” response. When this system is activated, there is an increase in heart rate, respiratory rate, and a slowing of digestive activity. The sympathetic nervous system has short preganglionic neurons which originate in the thoracolumbar column or T1 to L3 of the spinal cord. These sympathetic preganglionic neurons then synapse onto the cell bodies of long postganglionic neurons located in the sympathetic paravertebral or prevertebral ganglia. The postganglionic neurons release the neurotransmitter norepinephrine (NE) upon activation, which will bind α or β-adrenergic receptors present in target organs.

Conversely, the parasympathetic nervous system is referred to as the “rest and digest” response and when activated will lead to a slowing of heart rate, lowering of blood pressure, and increase in digestive activities. The parasympathetic nervous system has long preganglionic neurons which originate from the cranial-sacral column or the midbrain, pons, medulla and S2 to S4 of the spinal cord. The parasympathetic preganglionic neurons then synapse onto short postganglionic neurons that are located on or near target tissues. The parasympathetic postganglionic neurons release ACh, which binds muscarinic cholinergic receptors present in target organs.

As discussed, there are a number of similarities and differences between the sympathetic and parasympathetic nervous systems and the physiological responses they have on various target organs. However, the focus of this dissertation will be on the cardiovascular system.

Sympathetic Nervous System and Cardiac Electrophysiology

The heart is innervated by sympathetic postganglionic nerves that originate from the prevertebral ganglia. These nerves have the highest concentration of innervation at the base of the heart but they innervate all four chambers as well as the sinoatrial (SA) node, the atrioventricular (AV) node, bundle of His, and purkinje fibers (Kawano, Okada, and Yano 2003). As mentioned previously, during sympathetic activation, the neurotransmitter that is released is NE which binds α or β- adrenergic receptors (Jamali, Waqar, and Gerson 2017). β- adrenergic receptors are a class of cell surface receptors that play a crucial role in the body's response to epinephrine and NE. In the heart, 80% of the adrenergic receptors are β_1 and 20% being β_2 located in the cell membrane of cardiomyocytes (M R Bristow et al. 1986). When NE binds ß receptors in the heart this will lead to increases in heart rate (chronotropy), increased AV conduction, increased force of contraction (inotropy), and increased relaxation (lusitropy) to increase cardiac output.

ß adrenergic activation results in activation of the G-protein, $G_{\alpha s}$, that goes on to activate the membrane-bound protein adenyl cyclase (AC) resulting in production of the second messenger cyclic AMP (cAMP) and activation of the phosphatase protein kinase A (PKA) (Bers 2002a). PKA exerts its effect by phosphorylation of many different targets in the heart. In the SA node, PKA phosphorylates HCN4 channels in pacemaker cells leading to an increase in I_f current, which allows for faster depolarizations in pacemaker cells resulting in positive chronotropy (Liao

et al. 2010). Moreover, sympathetic activation and cAMP/PKA-dependent phosphorylation leads to increased I_{Ks} and I_{Kr} currents thereby shortening action potential durations (APD) (Kagan et al. 2002; Marx et al. 2002). Positive inotrophic effects during sympathetic activation are due to a rise in intracellular Ca^{2+} concentration which is a result of PKA-dependent phosphorylation of L-type calcium channels, phospholamban (PLN), and ryanodine receptors (RyR)(Bers 2002a). This rise in intracellular Ca^{2+} and subsequent positive inotropy is seen as an increase in the amplitude of the calcium transient and shortening of the calcium transient duration (CaTD). Phosphorylated PLN removes the inhibition on the SR Ca^{2+} ATPase (SERCA) pump present in the membrane of the sarcoplasmic reticulum (SR) (MacLennan and Kranias 2003). This allows for SERCA to pump Ca^{2+} into the SR thereby resulting in a positive lusitropy and typically a prolongation of the CaTD and shorter calcium decay times in larger mammals.

There are also adrenergic receptors present in vascular smooth muscle that influence blood pressure and subsequently heart rate via the baroreceptor reflex. When NE binds $ß_2$-AR in the vascular smooth muscle of peripheral arteries this will cause activation of the $G_{\alpha s}$ pathway and lead to vasodilation (Lymperopoulos et al. 2021; Sved 2009). This vasodilation results in a decrease in blood pressure resulting in less stretch of the wall of the aorta and carotid arteries. This decrease in stretch is sensed by baroreceptors present in the aortic arch and carotid bodies. The baroreceptors will then decrease their firing rate, which is sensed by the nucleus tractus solitarius (NTS) in the brainstem (Sved 2009; Pilowsky and Goodchild 2002). This leads to an increase in sympathetic outflow (more NE release) and an increase in heart rate. Conversely, when NE binds alpha adrenergic (α-AR) receptors present in the peripheral arteries and veins this leads to an increase in blood pressure and a decrease in heart rate. Binding of NE to α_1-AR

leads to activation of the $G_{\alpha q}$ pathway and an increase in phospholipase C (PLC), IP3, and intracellular Ca^{2+}; resulting in vasoconstriction of peripheral arteries and veins and ultimately an increase in blood pressure (Lymperopoulos et al. 2021). The baroreceptors sense this increased stretch of the aorta and carotid veins and increase their firing rate. The increased firing rate is sensed by the nucleus of the tractus solitarius (NTS) in the brainstem to activate the parasympathetic nervous system and inhibit sympathetic outflow and NE release to decrease heart rate.

Parasympathetic Nervous System and Cardiac Electrophysiology

The preganglionic nerve fibers of the parasympathetic nervous system that innervate the heart originate in the nucleus ambiguous and dorsal motor nucleus of the brainstem (Mitchell 1953). These fibers travel along the left and right vagus nerve, with the left vagus synapsing at short terminal ganglia to form the superior cardiac plexus or the inferior cardiac plexus. The nerves of the left vagus innervate the SA node to form the superior cardiac plexus and upon stimulation will lead to a decrease in heart rate (negative chronotropy). Nerves of the right vagus and left vagus synapse at terminal ganglia in the AV node and atria to form the inferior cardiac plexus. Stimulation of the inferior cardiac plexus slows down conduction from the atria to the ventricles through the AV node. Additionally, activation of the parasympathetic nervous system will result in a decrease in contractility of the ventricles (negative inotropy) which is enhanced in the presence of sympathetic stimulation.

In the heart, basal parasympathetic tone is high and is mediated through muscarinic receptors (Saternos et al. 2018). There are 5 muscarinic isoforms; however, the M_2 isoform is found in the

heart –specifically, the SA node, AV node, atrium, and ventricles. When ACh is released from parasympathetic nerve terminals of the superior cardiac plexus, it binds M_2 receptors in the membrane of SA nodal pacemaker cells causing activation of the G-protein, $G_{\alpha i}$. Activated $G_{\alpha i}$ causes dissociation of $G_{\beta\gamma}$ which then causes an increase in K^+ conductance through the $I_{k(ACh)}$ channels resulting in hyperpolarization of pacemaker potential, negative chronotropy, and slowing of AV conduction (Fu et al. 2006; Fleischmann et al. 2004). Negative chronotropic effects during parasympathetic activation are also a result of $G_{\alpha i}$ -dependent inhibition of AC in the AV and SA nodes (DiFrancesco 2010; DiFrancesco and Tortora 1991). Since AC is inhibited, this results in a decrease in cAMP production and subsequently a slowing of I_f current and diastolic depolarization. Moreover, AV conduction slows due to $G_{\alpha i}$ -dependent inhibition of AC/cAMP production which results in a reduction in the I_{ca} current shortening the CaTD and APDs. Lastly, parasympathetic activation on its own causes little to no effect on ventricular contractility but will attenuate sympathetic positive chronotrophy (Henning, Khalil, and Levy 1990).

Sympathetic Remodeling in Cardiovascular Disease

Sympathetic Remodeling and Cardiac Arrhythmias

Cardiovascular disease (CVD) is one of the leading causes of death in the United States (Mensah and Brown 2007). CVD is comprised of a range of disorders that include coronary artery disease, congenital heart disease, heart failure (HF), and myocardial infarction (MI). Additionally, CVD is exacerbated by environmental factors including smoking. In the healthy heart the structure of the myocardium, electrophysiology, and autonomic nervous system work together to coordinate

the electrical and mechanical phases of the cardiac cycle to ensure that blood is pumped efficiently to the rest of the body. Disruptions in any of these parameters can be pro-arrhythmic and may also lead to a reduction in cardiac output (CO); which if left untreated can develop into CVD. The sympathetic nervous system has been identified as a causative factor for arrhythmia in various disease states. Changes in the density of sympathetic nerves innervating the heart along with changes in adrenergic sensitivity can be particularly arrhythmogenic (R. T. Gardner et al. 2015; Ryan T. Gardner et al. 2016). In cases of new sympathetic nerve growth, innervation can become unbalanced or heterogenous thereby providing a substrate for abnormal rhythms to occur (L. S. Chen et al. 2007). Loss of sympathetic nerves or hypo-innervation can also create a heterogenous substrate and adrenergic supersensitivity (Park-Lee 2022). Moreover, alterations in the reuptake and release of NE can lead to pro-arrhythmic changes in sympathetic tone. For example, in the cases of inhibited NE reuptake, the increased circulating NE allows for a higher sympathetic tone and a lower threshold for ectopic activity. As such, in studies on the intact rabbit heart, it has been shown that heterogeneous application of NE increase the likelihood of premature ventricular contractions (PVC) (Myles et al. 2012).

During heart diseases such as MI and HF there is an increase in sympathetic tone and a reduction in parasympathetic output that can promote arrhythmias. This sympathetic hyperactivity occurs along with many changes such as electrophysiological remodeling, myocardial remodeling, neurotransmitter release, and sympathetic nerve density. Chronic nicotine exposure as occurs with smoking or vaping can also lead to sympathetic hyperactivity. Therefore, there may be similarities between autonomic remodeling that occurs in MI and HF with nicotine and as such nicotine exposure may also further exacerbate the hyperactivity in MI and HF.

Sympathetic Remodeling in Heart Failure:

Heart failure is a pathological syndrome that results when the heart is incapable of supplying sufficient blood flow to meet metabolic demands or accommodate systemic venous return. In 2021, the American Heart Association reported that the prevalence of HF is ~1.8% of the total US population or approximately 6 million Americans (Roger 2021). Approximately 20% of patients with HF die within 1 year of being diagnosed and 50% of those deaths are due to sudden cardiac death (SCD) (Tomaselli and Zipes 2004). HF is a progressive disease caused by a significant loss of functional myocytes after an injury. The most common causes for HF are myocardial infarction, hypertension, and diabetes (Kemp and Conte 2012). Certainly, MI alone can lead to myocardial weakening, it is the pressure overload from hypertension and excessive activation of renin-angiotensin system that trigger a cascade of events that result in harmful cardiac remodeling.

HF has typically been categorized by ejection fraction (EF) which is the amount of blood pumped from the heart in one heart beat. In a healthy heart, average EF ranges from 50 -70%. Whereas in HF with reduced ejection fraction, EF is less than 40% and is characterized by the ventricles having an impaired ability to contract (Murphy, Ibrahim, and Januzzi 2020). Conversely, HF with preserved EF have normal ventricular contraction but impaired relaxation and filling due to increased ventricular wall stiffness (Borlaug and Paulus 2011). In both types of HF there is a reduction in cardiac output (CO) that drives deleterious compensatory mechanisms.

Research suggests that sympathetic abnormalities may underlie the electrophysiological imbalances and cardiac remodeling observed in HF. Reduced CO activates the sympathetic nervous system as a compensatory mechanism to increase inotropy and lusitropy to improve CO. This excessive sympathetic activation or sympathetic hyperactivity results in elevated circulating catecholamines (Leimbach et al. 1986). Sustained elevated levels of catecholamines results in sustained over activation of ß-ARs. In order to combat this, cardiomyocytes downregulate the number of $ß_1$-AR receptors present at the membrane (Madamanchi 2007; M R Bristow et al. 1986; Michael R. Bristow et al. 1982). Additionally, studies have shown that in HF there is an upregulation of the negative ß-AR regulators $G\alpha_I$ and G-protein-coupled receptor kinase 2 (GRK2) further diminishing $ß_1$ -AR signaling (Ungerer et al. 1993; Kiuchi et al. 1993). Not only is ß-AR signaling altered in HF but there is electrophysiological remodeling that occurs that promotes lethal arrhythmias.

The electrophysiological changes that occur in HF involve modulation of ion channels and altered Ca^{2+} handling. Action potential prolongation is a common theme in HF experimental models and patients with HF (Coronel et al. 2013). Action potential duration (APD) prolongation is reflective of changes in the repolarization phase of the action potential which can be due to changes in K^+ currents. As such, studies have demonstrated a decrease in the densities of both the inward rectifier K^+ current (I_{K1}) and the transient outward K^+ current (I_{to}) in both animal and human models of HF (Kääb et al. 1996; Beuckelmann, Näbauer, and Erdmann 1993). Changes in I_{K1} can be particularly pro-arrhythmic because alterations in inward rectifying K^+ currents destabilizes the resting membrane potential making the myocardium more susceptible to spontaneous depolarization. Furthermore, APD prolongation in HF can also be a result of

increased late sodium currents (I_{NaL}) and has been shown in both animal models of HF and patients with HF (Coppini et al. 2013; Valdivia et al. 2005). Altered Ca^{2+} handling in HF contributes to delayed after-depolarizations (DAD). DADs result from elevated intracellular Ca^{2+} loading and spontaneous SR Ca^{2+} release which can activate the sodium calcium exchanger (NCX) and trigger an action potential (Lou, Janardhan, and Efimov 2012; Belevych et al. 2011; Pogwizd et al. 2001). As such, animal models of HF have shown that RyR-mediated SR Ca^{2+} leak and enhanced NCX activity increased the frequency of DADs (Belevych et al. 2011; Pogwizd et al. 2001).

Sympathetic Remodeling in Myocardial Infarction

Myocardial infarction often known as a "heart attack" stands as one of the prevailing instances of cardiovascular injury and carries a substantial risk of potential fatal ventricular arrhythmias. In the United States approximately 805,000 people suffer from a heart attack every year; of which 27% die before reaching the hospital (Boateng and Sanborn 2013) . Within the initial 72 hours following a MI, arrhythmias and conduction abnormalities arise in over 90% of patients, frequently leading to fatalities. The arrhythmias that occur post-MI are due to a combination of structural remodeling of the myocardium, electrical dysfunction, and remodeling of sympathetic nerves innervating the heart.

During an MI, one or more of the arteries supplying oxygen and nutrients to a region of the heart becomes occluded and the region becomes ischemic. If the occlusion is cleared then the reperfusion of blood flow to the region may prevent further damage; however, after MI the risk for arrhythmia or SCD increases drastically due to the cardiac remodeling in response to injury.

Structural remodeling of the myocardium occurs in the area that suffered ischemia. An acute inflammatory response occurs at the damaged region which leads to myofibroblasts laying down new extracellular matrix at the site of damage (van Nieuwenhoven and Turner 2013). Subsequently, the injured area undergoes fibrosis and formation of a scar thereby creating a heterogenous substrate that fosters DADs, reentry, and heightened ectopic automaticity (Kléber and Rudy 2004). Post-MI there is also remodeling of sympathetic nerve density within and around the scarred region.

In the area adjacent to the scarred region the myocardium can become hyper-innervated. This hyper-innervation is characterized by an excessive and disorganized growth of sympathetic nerves due to increased nerve growth factor (NGF) (Kimura, Ieda, and Fukuda 2012; Zhou et al. 2004). Conversely, the scarred region can become hypo-innervated as a result of increased chondroitin sulfate proteoglycans (CSPG) which block nerve re-growth (Ryan T. Gardner and Habecker 2013). This combination of hypo/hyper-innervation causes unbalanced levels of norepinephrine (NE) from sympathetic nerve terminals that is pro-arrhythmic. For example, sympathetic hyper-innervation leads to excess and non-uniform NE release from sympathetic nerves which increases the risk for abnormal rhythms (Myles et al. 2012).

Hypo-innervation in the scarred region of sympathetic nerves following MI is a predictor of detrimental ventricular arrhythmias (Ryan T. Gardner et al. 2016; Fallavollita et al. 2014; Boogers et al. 2010). In regions that have a loss of sympathetic nerves there is an increase in APD dispersion, altered Ca^{2+} handling dynamics, and ß -AR supersensitivity (Tapa et al. 2020; R. T. Gardner et al. 2015). Studies have shown that there is a decrease in GRK2 expression in

denervated hearts and an increase in GRK2 degradation post-MI (Penela et al. 2019; Yatani et al. 2006) which likely promote ß-AR supersensitivity. This is further supported by GRK2 knock-out mice that display supersensitivity of ß receptors (Raake et al. 2012). Diminished SERCA activity due to GRK2 downregulation has been linked to a decrease in SR Ca^{2+} content (Raake et al. 2012; Yatani et al. 2006). Decreased SR Ca^{2+} content has been shown to increase $Ca^{2+}{}_i$ and enhance NCX activity thereby promoting DADs. Moreover, hypo-innervation results in decreased I_{to} currents and increased susceptibility for ventricular fibrillation (Bai et al. 2008).

Moreover, excessive ß -AR stimulation can cause cardiomyocytes to become less responsive or desensitized to ß -AR stimulation. ß -AR desensitization can be due to downregulation of ß receptors and/or an increase in GRK2 (Lefkowitz, Rockman, and Koch 2000). As such, it was found that there was a decrease in ß-AR density in the remote noninfarcted region in patients post-MI (Ohte et al. 2012). Moreover, studies on patients with acute MI it was found that there was an elevation in GRK2 levels that correlated with diminished cardiac function (Santulli et al. 2011).

Sympathetic Remodeling and Nicotine Exposure

Cigarette smoking remains the leading cause of preventable disease, disability, and death in the United States. Additionally, smoking contributes significantly to the progression of coronary artery disease thereby increasing the risk for MI and ischemia-induced arrhythmias and sudden cardiac death. Short-term secondhand smoke (SHS) exposure increases the incidence for atrial fibrillation (AF) and ventricular tachycardia/fibrillation (VT/VF) in mice (C.-Y. Chen et al. 2008). Additionally, SHS exposure increased the susceptibility to Ca^{2+} and APD alternans which

may contribute to arrhythmias with SHS exposure (Z. Wang et al. 2018); however, what components of cigarette smoke contribute to alternans and SHS-induced arrhythmias are largely unknown. Interestingly, in 2021 11.5% of Americans over the age of 18 reported using cigarettes; however, these numbers have declined from 20.9% in 2005 (Cornelius 2023). Yet, as these numbers have declined, the prevalence for electronic cigarette (e-cigarette) usage has increased. In a recent study released by the Center for Disease Control and Prevention it was reported that e-cigarette unit sales increased by 46.6% between 2020 – 2022 (Ali 2023). In 2022, 16.5% of high school and 4.5% of middle school students reported using tobacco products within the last 30 days (Park-Lee 2022). Of the eight different commercial tobacco products assessed, electronic cigarettes (e-cigarettes) were the most used tobacco product among students. Within e-cigarettes the main component is nicotine. Nicotine has been associated with structural remodeling, changes in cardiac electrophysiology, alterations in autonomic regulation, and hemodynamic changes which can be pro-arrhythmic.

Nicotine can impact autonomic control of the heart because it binds nicotinic acetylcholine receptors (nAChR) that are present within the brain, the peripheral nervous system, and adrenal medulla (Grilli et al. 2005). In studies on rats using labeled norepinephrine, it was found that rats given nicotine for 10 days had a higher outflow of norepinephrine and lower outflow of acetylcholine than vehicle-treated rats in the hippocampus (Grilli et al. 2005), suggesting that the overall net effect from the central nervous system is sympathetically driven and that chronic nicotine exposure could lead to sympathetic hyperactivity.

In the peripheral nervous system, nicotine will bind nAChRs present on the adrenal glands and cause a release of epinephrine (E) and NE into circulation (Yokotani, Okada, and Nakamura 2002; Watts 1960; Dale and Laidlaw 1912). Additionally, nicotine can bind nAChRs present on the postganglia of sympathetic and parasympathetic nerves innervating the heart. This in turn will lead to a release of NE from sympathetic nerve fibers and binding of NE to $ß_1$-ARs preset on cardiomyocytes and increased cAMP production. Increased cAMP production results in increased HR, accelerated Ca^{2+} handling, increased contractility, and shortening of APD. Conversely, ACh will be released from parasympathetic nerve fibers which will inhibit cAMP production and oppose the sympathetic driven actions on electrophysiology and calcium handling. Under normal, healthy conditions the opposing sympathetic and parasympathetic branches are typically balanced and there may be imbalance with disease that can be pro-arrhythmic.

In the literature, nicotine has been linked to changes in cardiac electrophysiology and arrhythmogenesis. In a study on healthy non-tobacco using volunteers, it was found that volunteers that used e-cigarettes containing nicotine had a decrease in heart rate variability (HRV) compared to volunteers given e-cigarettes without nicotine and sham control (Moheimani, Bhetraratana, Peters, et al. 2017). In the clinical setting reduced HRV has been associated with increased risk for sudden cardiac death (SCD) in post-MI patients (Shekha et al. 2005; Malliani et al. 1994). Additionally, studies on isolated cardiomyocytes have shown that nicotine directly blocks I_{k1} (H. Wang, Yang, et al. 2000; H. Wang, Shi, et al. 2000). In previous studies from our lab we have shown that I_{k1} blockage leads to ectopic beats (Myles et al. 2015). Additionally, *in-vivo* administration of nicotine resulted in atrial and ventricular arrhythmias in

post-MI dogs (Yashima et al. 2000; Mehta et al. 1997). In a meta analysis study on nicotine replacement therapies it was found that there was an increased risk of rhythm disorders such as palpitations, bradycardia, and tachycardia (Mills et al. 2014; 2010).

Not only has nicotine been linked to changes in cardiac electrophysiology there are detrimental hemodynamic changes that occur and contribute to arrhythmogenesis. Nicotine can cause vasoconstriction of blood vessels in both the skin and coronary arteries (Benowitz and Fraiman 2017; Benowitz and Burbank 2016; Czernin and Waldherr 2003). This vasoconstriction leads to decreased coronary blood flow and increased risk for myocardial ischemia. Moreover, with vasoconstriction of peripheral veins there will be an increase in total peripheral resistance (TPR) and subsequently an increase in mean arterial pressure (MAP) or blood pressure (BP). As such, studies done in mice have shown that chronic nicotine inhalation leads to a transient increase in BP; as well as right ventricular hypertrophy and increased right ventricle wall thickness.(Oakes et al. 2020). Hypertension has long been associated with increased risk for CVD (Flint et al. 2019). Moreover, increased right ventricle mass has been associated with incident atrial fibrillation (Chatterjee et al. 2017).

Nicotine has been linked with structural remodeling of the myocardium. Specifically, it has been shown to be associated with increased atrial fibrosis which can contribute to atrial arrhythmias. For instance, in atrial tissue slices treated with nicotine it was found that there was an increased expression of collagen III, a major constituent of atrial fibrosis (Goette et al. 2007). Moreover, in a study on MI dogs it was found that nicotine caused a significant increase in atrial interstitial fibrosis and a mild increase in dogs with no MI (Miyauchi et al. 2005). Taken together this

increase in fibrosis interferes with conduction and creates an environment that is able to sustain atrial arrhythmias (Li et al. 1999).

Rabbit research models for studying cardiac disease:

Species Selection:

Animal models are often used to study mechanisms of human cardiac diseases; however, it is necessary to consider species differences across animal models when selecting the appropriate model for investigation. Larger animal models like the pig or dog have been used to study atherosclerosis, heart failure, and myocardial infarction (Zaragoza et al. 2011). The advantage of the pig or dog is that the size of the heart, cardiac anatomy, and beating rate closely resembles the human (Blackwell, Schmeckpeper, and Knollmann 2022). Moreover, there is enough cardiac tissue available for molecular or biochemical studies. Additionally, due to the larger size in the porcine or canine model, it is easier to study implantable devices or ablation methods. However, due to higher costs and longer gestation times this can be unaffordable, more so in the study of chronic disease states.

Indeed, most of the research on cardiovascular diseases has been done using mouse models. Mice are great models for cardiac diseases as they provide many benefits: they are cost-effective, have short gestation times, and can be easily genetically modified (Clauss et al. 2019; Pogwizd and Bers 2008). However, there are drawbacks when using mice in the study of cardiac diseases that should be considered. The mouse has a resting heart rate of 600 – 800 BPM which is substantially higher than humans which range from 60 – 100 BPM. Moreover, the cardiac

electrophysiology and Ca^{2+} handling is different between the mouse and human (Bers 2002b). The expression of K^+ channels is different in mice and humans, and as such, the shape and duration of the action potential (AP) is strikingly different. Humans have a long plateau phase in the AP which followed by repolarization that is governed by inward rectifying (I_{Kr}) and slow delayed rectifying (I_{Ks}) K^+ channels. Conversely, the AP in the mouse is sharp and repolarization is primarily driven by transient outward (I_{to}) current. Furthermore, because of the small size of the murine heart this may contribute to the self-termination of reentrant arrhythmias, which may prove challenging in arrhythmia studies (Blackwell, Schmeckpeper, and Knollmann 2022).

Rabbits have been used as a model to study several heart diseases such as: ventricular hypertrophy, heart failure, myocardial infarction, and arrhythmogenesis. Since rabbits are of intermediate size between mice and pigs or dogs they are more cost effective then larger models and can still be used to study medical devices and techniques (Pogwizd and Bers 2008). It is necessary to consider the animal model's anatomical size of the heart and species-dependent electrophysiology when studying detrimental arrhythmias like ventricular fibrillation. The effective size concept takes into account the anatomical size of the heart and arrhythmia pattern; such that it is the ratio between the size of the heart and the wavelength for reentry (Ellermann et al. 2021; Kang et al. 2016; Panfilov 2006). The effective size of the rabbit is ~0.9x that of the human; whereas the dog or pig are 1.4x and 1.6x, respectively making the effective size of the rabbit more comparable to the human then that of the pig or dog (Ellermann et al. 2021; Kang et al. 2016; Panfilov 2006). The cardiac electrophysiology and Ca^{2+} handling in the rabbit is more closely related to humans than mice, making them a more suitable model when studying the electrical remodeling and altered Ca^{2+} dynamics that occur in human cardiac diseases (Bers

2002b). The rabbit also has a long plateau phase in the AP and repolarization is driven mostly by I_{Kr} and I_{Ks} currents, much like in the human. Moreover, the Ca^{2+} handling dynamics in the rabbit are more similar to the human than the mouse. In mice, ~90% of the Ca^{2+} involved in contraction is released from the sarcoplasmic reticulum (SR) and is then re-sequestered back into the SR by the sarcoplasmic endoplasmic reticulum ATPase (SERCA) (Pogwizd and Bers 2008). However, in rabbits and humans, approximately 30% of Ca^{2+} enters through L-type Ca^{2+} channels and is extruded back out by the sodium-calcium exchanger (NCX). Therefore, due to their electrophysiological and calcium handling similarities with humans, rabbits are an ideal model to study cardiac diseases.

Isolated Cardiomyocytes:

Extensive work has been done using rabbit models on sympathetic remodeling in response to cardiac disease and injury. However, most of the mechanistic work has been done using isolated cardiomyocytes. The benefit of *in vitro* work on isolated cardiomyocytes is that it can be a high throughput method that allows researchers to control the environment and study the mechanism of cardiac diseases independent of other cell types and circulating factors (Lindsey et al. 2018a). This makes it an ideal model to mechanistically study the efficacy of drug-therapies, disease progression, or toxicity of chemicals.

One particular toxin that has been studied *in vitro* using isolated rabbit myocytes is nicotine. In newborn rabbits exposed to nicotine during gestation, it was found that nicotine exposure increased the amplitude of I_{Na} currents in right atrial cardiomyocytes (Ton et al. 2017).

Additionally, in adult sinoatrial (SA) nodal cells, nicotine produced negative chronotropy, inhibited I_{CaL} currents (Satoh 1997).

In vitro studies on sympathetic remodeling and hyperactivity have been performed by using pharmacological agonists/antagonists of ß-adrenergic receptors to mimic the sympathetic nervous system. The most common ß-adrenergic agonist that has been used is isoproterenol (ISO); however, the physiological neurotransmitters Norepinephrine (NE) and Epinephrine (Epi) have been used.

Research using adult rabbit ventricular myocytes has shown that sustained application of ISO leads to upregulation of L-type Ca^{2+} (I_{CaL}) channels (Akuzawa-Tateyama, Tateyama, and Ochi 2006). Furthermore, myocytes collected from failing rabbit hearts have shown that B_2-AR stimulation causes increases sarcoplasmic reticulum (SR) load and spontaneous SR release (DeSantiago et al. 2008). Moreover, NE application results in delayed after depolarizations (DAD), and triggered activity (Vermeulen et al. 1994). However, DADs in an isolated myocyte cannot be directly applied to focal arrhythmias in the whole heart; therefore, validation by *in vivo* or *ex vivo* animal models is crucial.

Langendorff Model:

The Langendorff rabbit heart model has been frequently used to study the mechanisms involved in cardiac electrophysiology under various disease states and conditions. In this model, hearts are extracted from the animal and then retrograde perfused with an oxygenated physiological saline solution through the aorta and the perfusate enters the coronary arteries ensuring that the heart is

properly oxygenated and perfused (Lindsey et al. 2018a; Bell, Mocanu, and Yellon 2011). The heart does not perform external work because perfusion is achieved by either constant flow or constant pressure. The advantage of this model is that a variety of physiological parameters, such as heart rate, myocardial contractility, and left ventricular systolic and diastolic function can be measured in a controlled environment. Furthermore, using optical mapping techniques it has become possible to obtain high resolution spatiotemporal recordings of the electrical activity of the heart (Kang et al. 2016). In this approach, excised hearts are loaded with voltage and/or calcium sensitive indicators to allow for analysis of changes in transmembrane potential and/or calcium transients.

The Langendorff-perfused rabbit heart model has been vital in the study of cardiac diseases such as myocardial infarction (MI) and heart failure (HF). In order to induce ischemic conditions in the Langendorff rabbit heart, perfusate flow to the heart is stopped for global ischemia or one of the coronary arteries is sutured for the set time and then released for ischemia/reperfusion (I/R) studies (Lindsey et al. 2018a). The advantage with this model is that accurate measurements of infarct size can be obtained, the acute electrophysiological effects of I/R can easily be analyzed, and enough tissue is available to perform molecular and biochemical assays. It has been shown in an I/R model that in the tissue surrounding an infarct, there is heterogeneous remodeling of the AP and Ca^{2+} cycling that occur that promotes ventricular arrhythmias (Chou et al. 2007). Additionally, in failing hearts, the Langendorff rabbit heart has been used to show that there is a non-uniform prolongation in the Ca^{2+} transient duration (CaTD) in the surviving myocardium (Ng, Cobbe, and Smith 1998).

Studies on sympathetic activation or hyperactivity in the Langendorff-perfused rabbit heart model have been done by adding sympathetic agonists to the perfusate. It has been shown that local NE administration was enough to overcome source-sink mismatch and trigger premature ventricular contractions (PVCs) and that local NE injections in conjunction with increased RyR sensitivity and decreased I_{K1} contribute to sustained focal ventricular arrhythmias (Myles et al. 2015; 2012). Additionally, in ischemic rabbit hearts it has been found that infusion of nicotine led to an increase in end-diastolic pressure, troponin, and noradrenaline (norepinephrine); suggesting that nicotine exacerbates ischemic hearts (Schrör, Zimmermann, and Tannhäuser 1998). However, it is challenging to get a true physiological representation of sympathetic activation in this model.

Innervated Heart Preparation:

The innervated heart preparation was originally introduced as an innovative approach to investigate physiological nerve stimulation (Ng, Brack, and Coote 2001a). During this technique, the intact heart can be extracted along with the spinal column and the posterior aspect of the ribs. This allows for direct stimulation of post-ganglionic sympathetic nerves that project out from the spinal cord. By removing the brainstem, this preparation allows for the evaluation of direct nerve stimulation on cardiac electrophysiology without interference from the brain or other reflexes. The advantage of this preparation is that it closely mimics physiological nerve stimulation compared to direct application of neurotransmitters to the perfusate. Moreover, the innervated heart preparation provides researchers with the opportunity to further investigate the heterogeneous changes in sympathetic nerves that may affect cardiac electrophysiology during

cardiovascular diseases (R. T. Gardner et al. 2015). Lastly, this preparation allows researchers the ability to study direct sympathetic nerve activation on cardiac electrophysiology with simultaneous changes in heart rate, which is not possible when using pharmacological methods.

The intact innervated heart preparation has been performed in both rabbits and mice (Tapa et al. 2020; L. Wang et al. 2019; Francis Stuart et al. 2018; Ng, Brack, and Coote 2001a). In the rabbit innervated heart model, it has been shown that stimulation of sympathetic nerves resulted in a gradual increase in heart rate and shortening of atrioventricular (AV) conduction; whereas direct stimulation of the vagus nerve lead to an abrupt decrease in heart rate and lengthening of AV conduction (Ng, Brack, and Coote 2001a). Furthermore, Wang and colleagues conducted dual optical mapping using voltage and calcium-sensitive indicators to examine the effect of sympathetic nerve stimulation (SNS) on action potential and calcium transient dynamics in both the innervated mouse and rabbit hearts (2019). It was found that in both species there was an expected increase in heart rate with SNS. Yet, within the innervated rabbit heart, SNS resulted in shortening of action potential duration (APD) and calcium transient duration (CaTD), and a reversal in the repolarization wavefront. Conversely, in the innervated mouse heart, SNS caused shortening of CaTD, an initial prolongation of APD before shortening, and very little change in the direction of repolarization. The innervated heart preparation has also been used to study age-related changes in sympathetic nerve structure and function and how those changes effect cardiac electrophysiology and Ca^{2+} handling. In aged mouse hearts is has been shown that there is a decreased responsiveness to SNS. Specifically, sympathetic nerve stimulation thresholds (as measured by percent change in heart rate) were higher and there is little change in heart rate, APD, or CaTD with SNS in aged compared to young hearts (Francis Stuart et al. 2018).

However, despite little previous work being done using the innervated heart preparation to study chronic disease states and sympathetic remodeling, the innervated rabbit heart preparation is an invaluable method. It allows for more physiological stimulation of sympathetic nerves and NE release/reuptake compared to the isolated Langendorff preparation which uses ß-AR agonists to mimic the sympathetic nervous system. Furthermore, the innervated rabbit heart preparation provides an opportunity to investigate the remodeling of sympathetic nerves and corresponding effect that has on cardiac electrophysiology.

Scope of Dissertation:

There is much preclinical and clinical data that has demonstrated the detrimental effects of sympathetic remodeling that occurs in response to cardiac injury or cardiovascular disease (CVD). Yet, despite the wealth of knowledge on sympathetic remodeling currently available, the influence of sympathetic hyperactivity on cardiac electrophysiology in a more human-like model, the rabbit, is largely unknown. Moreover, to what extent chronic nicotine exposure influences autonomic regulation of the heart and cardiac electrophysiology is not well understood. Thus, the objective of this dissertation is to determine the effect of myocardial infarction and chronic nicotine exposure on sympathetic remodeling and hyperactivity in the innervated rabbit heart. Chapter 2 addresses the role of chondroitin sulfate proteoglycans (CSPG) in sympathetic nerve outgrowth after myocardial infarction in the rabbit heart and resulting electrophysiological consequences. This study aims to confirm previous findings of the presence of CSPGs in the sympathetic *hypo*-innervated infarct region of the mouse heart, something that has not yet been demonstrated in larger animal models. Chapter 3 focuses on the effect of

chronic nicotine exposure on sympathetic remodeling and cardiac electrophysiology. This study aims to elucidate the mechanisms by which chronic nicotine exposure leads to Ca^{2+} mishandling, electrophysiological changes, and potential arrhythmogenesis. Chapter 4 summarizes the main findings and its impact on cardiac electrophysiology, provides significance in the understanding of sympathetic hyperactivity and CVD, and potential future directions.

Chapter II: Sympathetic Responsiveness and Arrhythmia in a Rabbit Model of Myocardial Infarction

Abstract:

Introduction: Hypo-innervation of the cardiac sympathetic nerves is associated with worse cardiovascular outcomes, including ventricular arrhythmias and sudden cardiac death. Rodent models of myocardial infarction (MI) show that chondroitin sulfate proteoglycans (CSPGs) inhibit sympathetic reinnervation post-MI and that regional hypo-innervation causes supersensitivity of ß-adrenergic receptors and increased arrhythmia susceptibility. Our goal for this study was to use a rabbit model of MI to determine if CSPGs and associated sympathetic hypo-innervation are present post-MI and the resulting electrophysiological responses to sympathetic stimulation.

Methods: Fully innervated hearts from rabbits that underwent MI (N=8) or sham (N = 4) surgery were optically mapped using voltage- (RH237) and calcium-sensitive (Rhod2-AM) indicators to evaluate action potentials and intercellular Ca^{2+} transients. Sympathetic nerve stimulation (SNS) was performed with electrical stimulation (8Hz, 10V) of the spinal cord at the 1^{st}-3^{rd} thoracic vertebra. ß-adrenergic stimulation was performed using isoproterenol (ISO, 30nM -500nM). Immunohistochemistry was performed to evaluate the presence of CSPGs. Sympathetic nerve density was quantified by tyrosine hydroxylase (TH+) staining.

Results: CSPG-positive signal was present in the infarct and border zone of all (6/6) MI hearts, and no CSPG fluorescence was observed in remote regions. Sympathetic nerve density was significantly reduced in the infarct region compared to remote (6.412 ± 2.784% vs. 0.5582 ± 0.3966%, P=0.0005). MI hearts had an increase in action potential duration (APD) dispersion with SNS, whereas sham hearts did not. With SNS, susceptibility to ventricular tachycardia/fibrillation (VT/VF) was increased in MI compared to sham (5/8 vs 0/0). SNS significantly shortened APD_{80} values compared to baseline in all regions of MI hearts. Application of ISO significantly shortened APD_{80} and Ca^{2+} transient duration ($CaTD_{80}$) compared to baseline values in both MI and Sham hearts, with MI hearts having a significantly greater relative shortening of $CaTD_{80}$ with ISO compared to sham (-42.60 ± 1.705% vs -33.04 ± 4.665%, P=0.02).

Conclusions: We found that CSPGs are present in the infarct region and are associated with sympathetic hypo-innervation, suggesting that sympathetic remodeling post-MI may be similar in rodents and larger mammals. Following physiological sympathetic nerve stimulation, there is an increase in APD dispersion and increased susceptibility for VT/VF post-MI. Despite a significant reduction in sympathetic nerve density, MI hearts remain responsive to both physiological sympathetic nerve stimulation and ISO, potentially through preserved or elevated ß-adrenergic responsiveness.

Abbreviations:

AP (action potential), APD (action potential duration), APD_{80} (action potential duration at 80% repolarization), ARI (action recovery interval), CaT (calcium transient), CaTD (calcium transient

duration), $CaTD_{80}$ (calcium transient duration at 80% repolarization), CSPG (chondroitin sulfate proteoglycans), HR (heart rate), ISO (isoproterenol), MI (myocardial infarction), Pacing cycle length (PCL), PTPσ (protein tyrosine phosphatase receptor sigma), SNR (signal to noise ratio) SNS (Sympathetic nerve stimulation), ß-AR (ß adrenergic receptors), TH (tyrosine hydroxylase), Trise (AP rise time), VF (ventricular fibrillation), VT (ventricular tachycardia)

Introduction:

Myocardial infarction (MI) stands as one of the prevailing causes of cardiovascular injury and carries a substantial risk of potential fatal ventricular arrhythmias (Adabag et al. 2021; Weir, McMurray, and Velazquez 2006). Following MI, there is significant remodeling of the cardiac sympathetic innervation as a result of the ischemic injury. In particular, sympathetic hypo-innervation of the heart post-MI has been linked to worse cardiac outcomes, including cardiac arrhythmias and sudden cardiac death (Fallavollita et al. 2017; 2014; Nishisato et al. 2010). Experimental studies have indicated that non-uniform sympathetic nerve density along with changes in adrenergic sensitivity may be especially arrhythmogenic (Ajijola et al. 2017; Ryan T. Gardner et al. 2016; R. T. Gardner et al. 2015).

Previous work has shown that chondroitin sulfate proteoglycans (CSPGs) present in the infarct region inhibit sympathetic nerve regrowth in the infarct and the adjacent myocardium in rodent models of reperfused MI (R. T. Gardner et al. 2015; Ryan T. Gardner and Habecker 2013). More recent findings have indicated that sulfation of CSPGs plays a key role in the inhibition of sympathetic reinnervation post-MI (Blake et al. 2023; 2022a). Additionally, it has been shown

that disrupting CSPG 4,6 tandem sulfation allows for sympathetic nerve regrowth in the infarct region and decreased arrhythmia susceptibility for up to 40 days after MI (Blake et al. 2023; 2022a).

Electroanatomical mapping of the hearts from MI patients has shown that areas of sympathetic hypo-innervation are also present in the human heart and are associated with ß -adrenergic supersensitivity and increased dispersion of the activation recovery interval (ARI, a surrogate for action potential duration [APD]) during sympathetic stimulation (Vaseghi et al. 2012a). Similarly, we have shown in post-MI mouse hearts that hypo-innervation leads to ß -adrenergic supersensitivity, Ca^{2+} mishandling, increased APD dispersion, and increased arrythmia susceptibility (R. T. Gardner et al. 2015). Our more recent findings have indicated that these same adrenergic and electrophysiologic changes can occur in areas of sympathetic hypo-innervation even in the absence of ischemia or MI (Tapa et al. 2020).

Most of this previous experimental work has been performed in mice, where cardiac electrophysiology is quite different from that of larger species, including human (Blackwell, Schmeckpeper, and Knollmann 2022; Ripplinger et al. 2022). However, cardiac electrophysiologic properties and Ca^{2+} handling in the rabbit heart are considerably more similar to humans (Bers 2002a). Moreover, the anatomical size of the rabbit heart and arrhythmia patterns are more closely related to those in human and allow for the study of sustained ventricular arrhythmias, which may be less prevalent in smaller rodent hearts (Ellermann et al. 2021; Kang et al. 2016; Panfilov 2006). Therefore, we sought to use a rabbit model of reperfused MI to determine if CSPGs and associated sympathetic hypo-innervation are present following MI

and the resulting electrophysiological responses to sympathetic stimulation. Physiological sympathetic nerve stimulation was performed in a fully innervated isolated rabbit heart preparation along with optical mapping and ECG analysis.

Methods:

Ethical Approval

All procedures involving animals were approved by the institutional animal care and use committee of the University of California, Davis (protocol #20991), and adhered to the *Guide for the Care and Use of Laboratory Animals Published by the National Institutes of Health* (NIH Publication No. 85-23, revised 2011).

Animals and Surgery

New Zealand White (NZW) rabbits (body weight=2.6 – 3.0 kg, n= 22) were purchased from Charles River Laboratories and were acclimated for at least 1 month before study. Rabbits were randomly assigned to sham or myocardial infarction (MI) surgery at a ratio of ~1:3 to account for MI-associated mortality, resulting in N=5 (3M, 2F) shams and N=17 (9M, 8F) MIs. For surgery, rabbits were sedated with butorphanol and/or acepromazine. Anesthesia was induced with ketamine and diazepam via ear vein catheter and maintained with inhaled isoflurane (~2%) via a ventilator for the duration of surgery. Rabbits were shaved and a ~4cm incision was made at the 4th intercostal space. A chest retractor was placed to expose the heart and lung. The pericardium was carefully pulled apart with forceps to visualize the left coronary artery. The descending branch of the left circumflex artery was ligated midway between the apex and base with a suture

for 45-60 min (Lindsey et al. 2021; 2018b). During the ligation, the retractor was removed, and the chest was closed. A bolus of lidocaine (0.5-1 mg/kg) was IV infused before ligation to prevent ventricular arrhythmias. In the event of ventricular fibrillation (VF), rabbits were given an additional bolus (0.5 mg/kg, IV) of lidocaine and the hearts were manually massaged by hand for recovery. Sham surgeries were performed by passing the suture under the coronary artery without ligation. Heart rate (HR), body temperature and blood pressure were monitored during surgery. Body temperature was maintained at 37°C by placing rabbits on a temperature-controlled warming pad. Ringer's lactate was given via IV infusion during surgery to ensure adequate hydration. Enrofloxacin (5 mg/kg) was given once to prevent infection. Buprenorphine (0.05-0.1 mg/kg) was given immediately post-surgery and then two times per day for 48 hours. Meloxicam was given once daily for 5 days.

Sample Sizes

Of the N=17 MI operated rabbits, N=10 (7M, 3F) survived. Although more males survived than females, there was not a statistically significant sex difference in survival rate (Fisher's exact, P = 0.1534). All deaths occurred due to ventricular arrhythmias during reperfusion even with lidocaine administration and defibrillation. Of the N=10 surviving MIs, N=8 (2 females, 6 males) innervated hearts were successfully perfused but remained fragile throughout the perfusion and mapping protocol; therefore, not all measurements or pacing protocols were performed in every heart. Due to the innervated preparation, it was sometimes not possible to visualize the infarct region within the mapping field of view. These factors all influenced N-numbers for each dataset and N-numbers are detailed within each figure legend.

Innervated Heart Preparation

Innervated rabbit hearts were prepared as previously described (Wang, 2019; Ng 2001). Briefly, on days 9-11 post-surgery, rabbits were intravenously administrated heparin (1000 IU, Fresenius Kabi USA, IL), then an overdose of pentobarbital sodium (>100 mg/kg). Upon deep anesthesia, the chest was quickly opened by incisions on both sides of the thoracic cavity and the front of the ribcage was removed. The pericardium was gently pulled apart and away from the heart and hearts were incubated with ice-cold cardioplegia (in mmol/l: NaCl 110, CaCl2 1.2, KCl 16, MgCl2 16, and NaHCO3 10). The descending aorta was then cannulated with 8-gauge cannula to flush hearts with ice-cold cardioplegia. The heart and posterior rib cage were removed by cutting the cervical spine at C1 and the thoracic spine at T12. The preparation was then dissected from surrounding tissues and submerged into ice-cold cardioplegia. The innervated heart preparation was moved to a glass-jacketed chamber and perfused via the descending aorta with Tyrode's solution at 37°C: (in mmol/L: NaCl 128.2, $CaCl_2$ 1.3, KCl 4.7, $MgCl_2$ 1.05, NaH_2PO_4 1.19, $NaHCO_3$ 20 and glucose 11.1). Perfusion pressure was maintained at 40-60 mmHg by adjusting the flow rate (~100-120 ml/min). Three Ag/AgCl needle electrodes were positioned in the bath (two in the thoracic cavity and one grounded in the chamber) for continuous ECG recording.

Dual Optical Mapping

Optical mapping of *Vm* and intracellular Ca^{2+} was performed as previously described (Ripplinger et al. 2022; L. Wang et al. 2019; Myles et al. 2012). The excitation-contraction uncoupler blebbistatin (Tocris Bioscience, Minneapolis, MN; 20μM) and the nondepolarizing skeletal muscle paralytic vecuronium (Cayman Chemical, Ann Arbor, MI, USA; 5μM) were added to the perfusate to eliminate motion artifact due to sympathetic nerve stimulation during optical

recording. Hearts were then loaded with 50uL of RH237 (Molecular Probes, Eugene, OR), a membrane voltage-sensitive dye, dissolved in 1mg/mL DMSO. Rhod-2 AM, an intracellular calcium indicator (Molecular Probes, Eugene, OR), was loaded in 0.5mL of DMSO containing 10% pluronic acid. The anterior epicardial surface of the left ventricle (LV) was excited using two LED light sources centered at 531 nm and band-pass filtered from 511 to 551 nm (LEX-2, SciMedia, Costa Mesa, CA). Fluorescence emitted from the anterior epicardium was collected using a THT- macroscope (SciMedia). The wavelengths were divided using a dichroic mirror at 630nm. The longer wavelength, which contained the Vm signal, was filtered using a longpass filter at 700nm. The shorter wavelength, carrying the intracellular Ca^{2+} signal was filtered using a 32nm bandpass filter centered at 590nm. Image acquisition took place at a rate of 1 kHz within a field of view measuring 31x31 mm (100x100 pixels) using complementary metal oxide cameras (MiCam Ultima-L, SciMedia Costa Mesa, CA).

Sympathetic Nerve Stimulation, Cardiac Pacing Protocol, and ß-Adrenergic Responsiveness

For sympathetic nerve stimulation (SNS), a 6F quadripolar catheter (2 mm electrode, 5 mm spacing) was inserted into the spinal cord to T1-T3 for SNS as previously described (L. Wang et al. 2019; Ng, Brack, and Coote 2001b). According to our previous studies, rabbit hearts have a strong response to SNS in a range of 5 -15 Hz and 5-10V for no longer than 60s as measured by robust changes in heart rate (L. Wang et al. 2019).Thus in this study, hearts were stimulated with SNS at 8Hz and 10 V for 13s (with ventricular pacing) or for 60 s in sinus rhythm. For ventricular pacing, a customized bipolar pacing electrode was placed on the surface of the mid/base right ventricle for cardiac pacing. Baseline electrophysiological parameters were measured during LV epicardial pacing at a pacing cycle length (PCL) of 200 ms with or without

SNS. To assess indicators of arrhythmia with SNS, hearts were stimulated with SNS for 60s. To induce ventricular tachycardia (VT) or ventricular fibrillation (VF), hearts were paced at progressively faster PCLs in 20 ms steps until loss of capture or induction of VT/VF. Responsiveness to β-adrenergic stimulation was assessed with isoproterenol (ISO; 30nM – 500nM) which was added to the perfusate.

Optical Mapping Data Analysis

Data analysis was conducted using the software *Optiq* (Cairn, UK) and *Electromap* (O'Shea et al. 2019)as described in our previous studies (Caldwell et al. 2023; Tapa et al. 2020). Briefly, action potential duration (APD) or Ca^{2+} transient duration (CaTD) were calculated as 80% repolarization minus activation time. APD dispersion was determined by dividing the range between the 5^{th} and 95^{th} percentiles of APDs within the field of view by the median APD value. The infarct region was defined as a signal to noise ratio (SNR) between 5 – 10 and an AP rise time (Trise) greater than 15 ms (L. Wang et al. 2020). The remote region was defined as an area of similar size but far from the infarct region and toward the base of the heart. The corresponding anatomical regions were selected in sham hearts.

Histology and Immunohistochemistry

Following optical mapping, a subset of MI hearts (N = 6) was fixed in 4% paraformaldehyde, and placed in 30% sucrose overnight. Short axis sections (approx. 2 mm) were frozen in optimal cutting temperature (OCT) medium for sectioning. Each heart was sectioned from base to apex at 2 mm spacing (6 sections/heart) before being embedded in OCT and then frozen/stored at -80°C.

The OCT block was then cryo-sectioned in 10 µm thickness and each section was thaw-mounted onto positively charged slides (Acepix Biosciences Inc Hayward, CA, USA).

CSPG and Tyrosine Hydroxylase Staining:

Immunohistochemistry was performed as previously described (Blake et al. 2022a; Tapa et al. 2020; Francis Stuart et al. 2018; R. T. Gardner et al. 2015). In brief, slides were rehydrated with phosphate buffered saline (PBS) and incubated in sodium borohydride (10 mg/mL; 3 x 3min). Slides were then blocked with 2% bovine serum albumin (BSA) in PBS containing 0.3% Triton X-100 (PBS-T) for 1 hr and probed with primary antibody that detect CSPG (1:300, Sigma CS-56) and Tyrosine Hydroxylase (1:300, EMD Millipore) overnight. Secondary antibodies (Goat Anti-Mouse; Goat Anti-Rabbit 1:500) conjugated to Alexa Fluor® 488 or to Alexa Fluor® 568 were applied to the samples for 90 mins. Following incubation with secondary antibody, glycerol in PBS (1:1) was used to mount coverslips. Images were acquired on a Nikon Eclipse Ni microscope at 10 x magnification with a FITC or TRITC filter (Ex 470/40 or 525/50 nm). Whole sections were imaged at 4x magnification for an overview. A minimum of 5 images were taken of the infarct, border and remote zone of each section to confirm the presence of CSPGs. Tyrosine hydroxylase (TH) quantification was analyzed with Nikon NIS-Elements Basic Research Microscope Imaging Software to determine the percentage tissue area that was TH +. Percent fiber density was defined as the ratio of TH+ fiber area to total tissue area.

Histology

Masson's trichrome staining was performed as previously described (Tapa et al. 2020) and according to the manufacturer's instructions (Trichrome Stain [Masson] Kit, Millipore-Sigma).

Statistics

Data are expressed as means ± SD and analyzed using GraphPad Prism 9. On data with multiple comparisons, two-way ANOVA with repeated measures followed by Sidak's post-hoc test was utilized. Comparisons between two groups were conducted using student's unpaired *t*-test. Fisher's exact test was used for comparing VT/VF rate. P-values <0.05 were considered statistically significant.

Results

CSPG and Sympathetic Nerve Density:

Previous studies using an ischemia-reperfusion model of MI in rodent hearts indicated that sympathetic nerve re-growth in the infarct region was prevented due to the presence of CSPGs (Blake et al. 2023; R. T. Gardner et al. 2015; Ryan T. Gardner and Habecker 2013). To determine whether CSPGs are present in larger mammals post-MI, the presence of CSPGs was evaluated and found in the infarct and border regions of all 6 post-MI rabbit hearts evaluated (Fig 1). No hearts showed any CSPG-positive signal outside of the infarct and border zone.

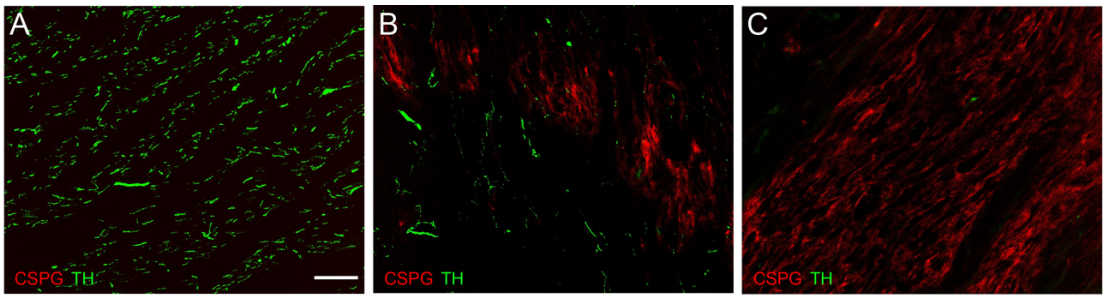

Figure 1: CSPG production in the infarcted rabbit heart. Sections from Mi rabbit hearts stained for CSPG (red) and TH (green) in (A) Remote, (B) Border and (C) Infarct zones. Scale bar, 100 μm. Similar results obtained in sections from 6 MI hearts.

Tyrosine hydroxylase labeling was also performed and indicated visible sympathetic nerve fiber loss in the infarct region (red) compared to the remote region (yellow) (Fig 2A). The location and size of infarct regions were verified by Masson's Trichrome staining of sister sections (Fig 2B). Sympathetic nerve density was quantified and indicated that the remote region had a significantly higher percent area that was TH+ compared to the infarct region (Fig 2C; 6.412 ± 2.784% vs. 0.5582 ± 0.3966%, P=0.0005).

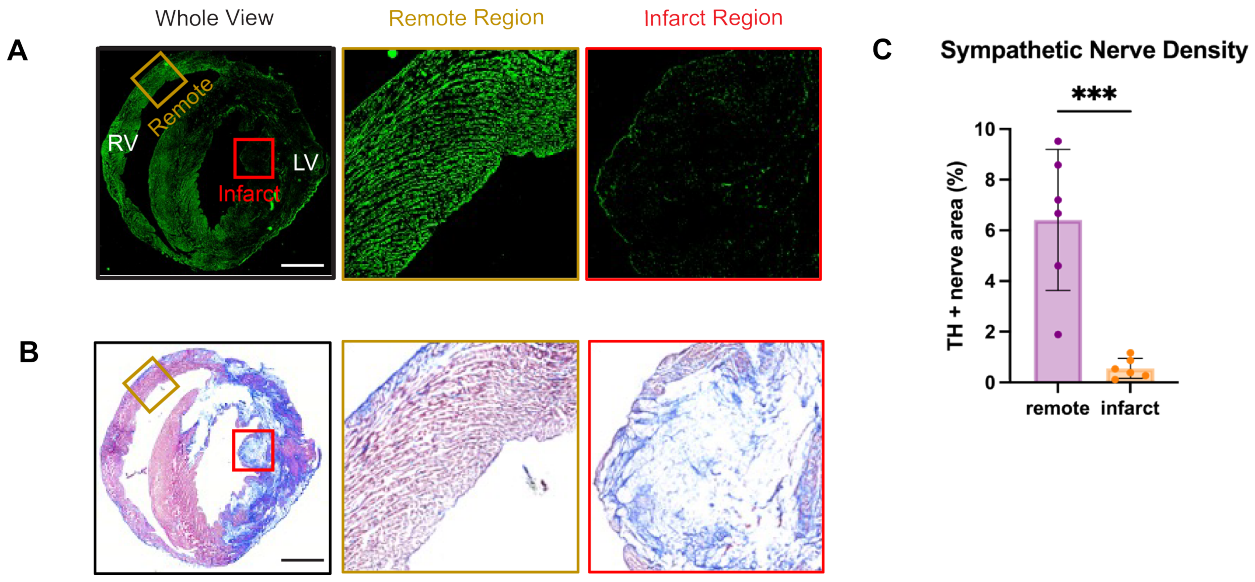

Figure 2: Sympathetic nerve density and masson's trichrome in the whole view, remote region, and infarct region of MI hearts. (A) Representative immunofluorescence images of TH+ labeling (B) Representative images of Masson's trichrome staining; fibrosis indicated in blue and myocardial tissue in red (C) Average sympathetic nerve density (presented as % area, data are means ±SD), N= 6 MI hearts, ***P<0.001. Scale bar, 100 μm

Effect of SNS on Heart Rate, Electrophysiology, and Arrhythmogenesis post-MI:

To determine the effect of SNS on electrophysiological parameters, HR, APD_{80}, APD_{80} dispersion, and VT/VF incidence were measured throughout 60 sec of SNS while hearts remained in sinus rhythm (Fig. 3A-C). In both groups, HR significantly increased by 10 sec of SNS (Sham: 155.38 ± 5.37 BPM vs 249.24 ± 21.12 BPM P = 0.02; MI: 140.40 ± 20.43 vs 231.06 ± 48.13 BPM P= 0.006) and remained relatively stable for the remainder of stimulation. Sham hearts had a slight trend for faster HRs compared to MI, but the difference between groups was not statistically significant (Fig 3A). Both groups also demonstrated shortening of APD_{80} over time with SNS, with a trend for longer APD_{80} in the MI group throughout SNS (Fig 3B).

Interestingly, while dispersion of APD_{80} remained constant in Sham hearts, APD dispersion gradually increased in MI hearts, and peaked at 40s of SNS (Fig 3C). To assess susceptibility to VT/VF, rapid ventricular pacing was performed during short-duration (13 sec) SNS. Fig 3D shows a representative ECG trace in which VT was induced during pacing and SNS in an MI heart. In this example, the VT persisted for approximately 1 min following the cessation of pacing and SNS, at which time it spontaneously terminated (presumably as catecholamine levels decreased post-SNS). Overall, 5/8 MI hearts had VT/VF compared to 0/4 sham hearts (Fig 3E).

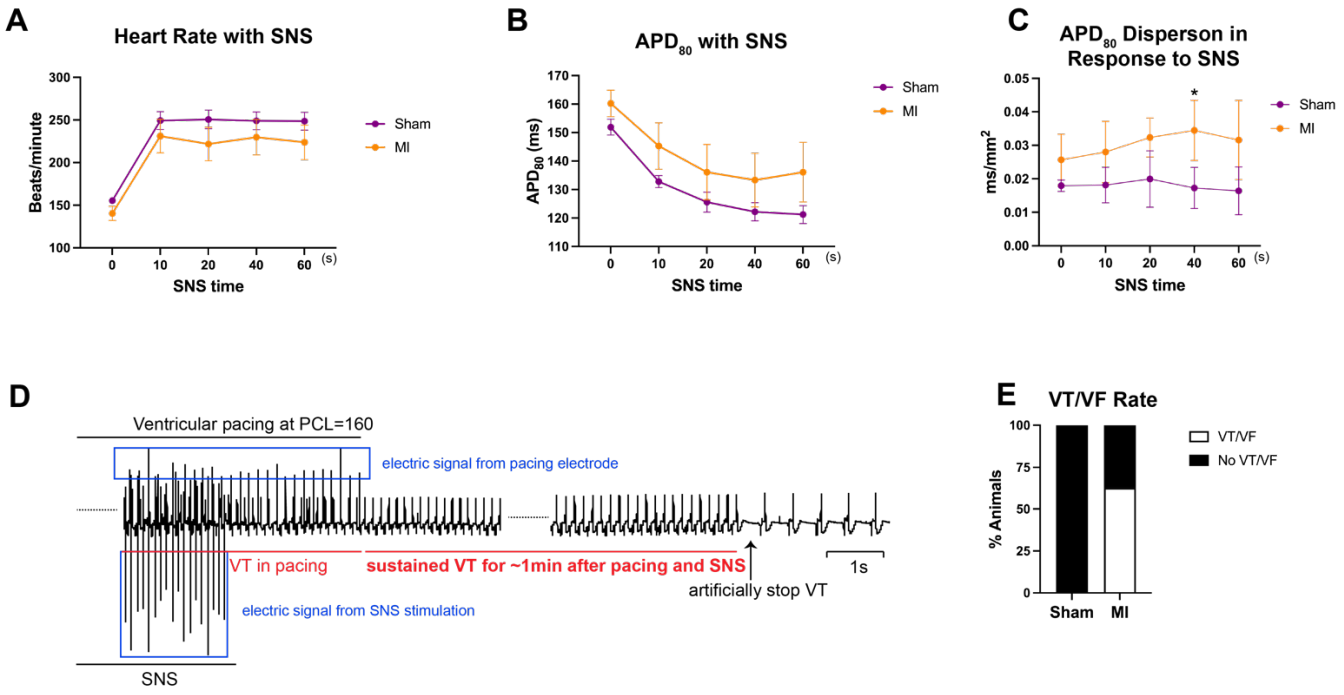

Figure 3: Effect of SNS on APD, APD dispersion, and VT/VF rate in sham and MI hearts

(A)Changes in heart rate with SNS N= 4-6/group (except T = 20, N=4-5/group) (B) Changes in APD_{80} with SNS N = 3-5/group 0-40s and 3-4/group 60s (C) APD dispersion in response to SNS N= 3-5/group (Note * compared to groups time 0 value) (D) Example trace of ventricular tachycardia (E) Rate of VT or VF N=4-8/group. *P<0.05(A – C) Two-way ANOVA with multiple comparisons (E) Fisher's exact test

To further determine the effect of SNS, rate-matched data from whole heart, remote, and infarct regions with and without SNS were assessed. Figure 3A shows photographs of the innervated rabbit heart preparation along with maps of Trise and SNR, which were used to define the infarct and remote regions for analysis (see Methods). Hearts were initially paced at baseline (PCL = 200ms) and then at the same PCL with SNS. SNS significantly shortened APD_{80} in the whole heart, remote, and infarct regions of MI hearts compared to baseline values but APD_{80} changes were not statistically significant in sham hearts (Fig 4 B-D). $CaTD_{80}$ values did not significantly change with SNS in any region in either group when compared to baseline values (Fig. 4 E-G). However, MI hearts had significantly shorter $CaTD_{80}$ compared to sham in the whole heart (Fig 4E, 129.0 ± 3.441ms vs 134.7 ± 1.397ms, P=0.02) and remote region (Fig 4F, 129.1 ± 3.704 ms vs 134.9 ± 1.295ms, P=0.02) with SNS.

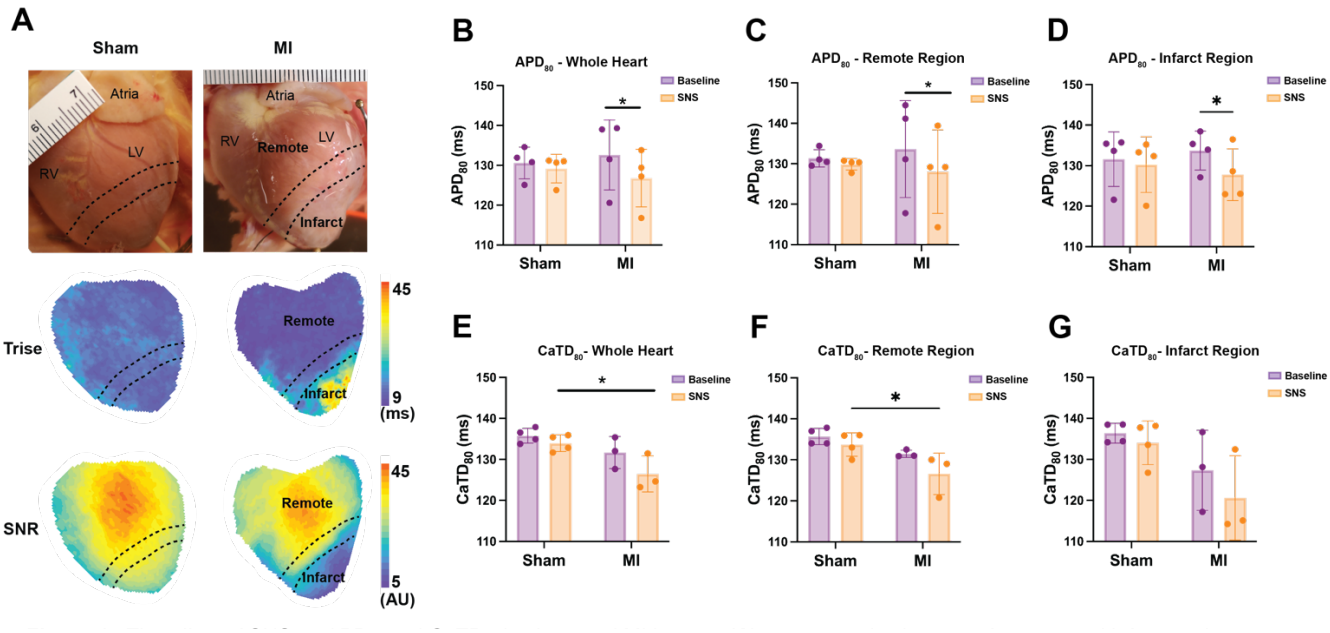

Figure 4: Effect of SNS on APD_{80} and $CaTD_{80}$ in sham and MI hearts (A) Representative images of remote and infarct region as defined by CaT rise times (CaT) and signal to noise ratio (SNR). Infarct region was defined by having a SNR between 5 – 10 and a

Trise greater than 15ms, remote region was of similar size and towards the base. APD80 changes with SNS in the (B) whole heart (C) remote region and (D) infarct region. $CaTD_{80}$ changes with SNS in the (E) whole heart (F) remote region and (G) infarct region. Data are means ±SD, N= 3-5 hearts/group, *P<0.05, by two-way ANOVA with repeated measures.

β-adrenergic Responsiveness:

The electrophysiological changes observed in response to SNS may arise from modified sympathetic nerve density or function (e.g., local NE release), altered responsiveness of cardiomyocytes to β-adrenergic stimulation, or a combination of both. Therefore, to specifically evaluate β-adrenergic responsiveness of cardiomyocytes, isoproterenol (ISO) was added to the perfusate. Fig 5A & C shows APD_{80} and $CaTD_{80}$ values measured immediately prior to the addition of ISO (baseline) and after ISO was added and allowed to reach a steady state. To account for differences in baseline values, the percent change in APD_{80} and $CaTD_{80}$ with ISO was also calculated (Fig 5B & D). Both sham and MI hearts had significantly shorter APD_{80} and $CaTD_{80}$ compared to their baseline values, with MI hearts having a significantly greater relative shortening of $CaTD_{80}$ with ISO compared to sham hearts (-42.60 ± 1.705% vs -33.04 ± 4.665%, P=0.02).

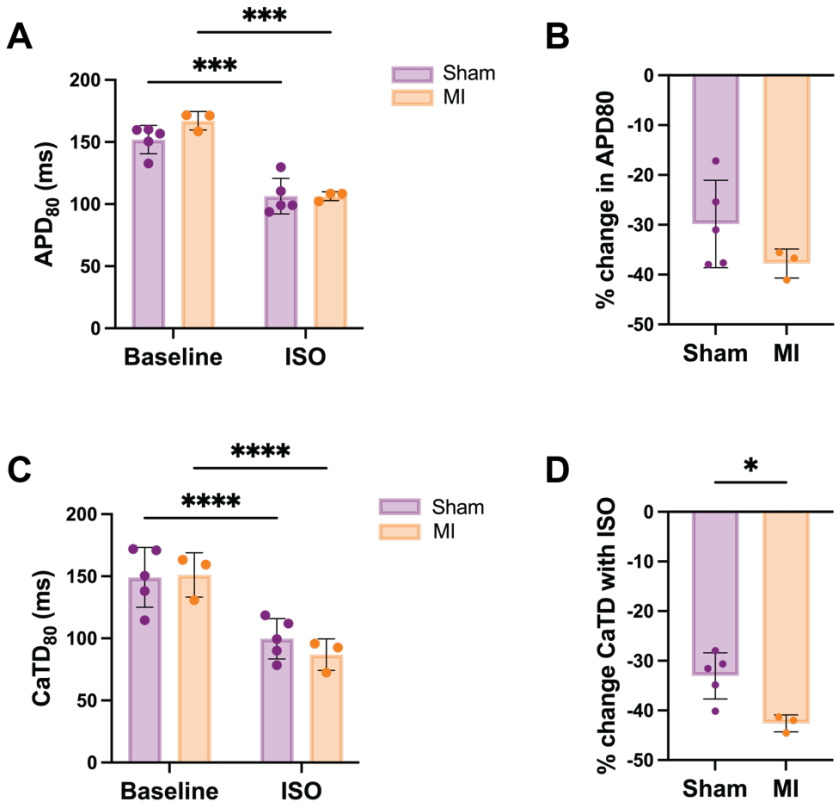

Figure 5: The effect of Isoproterenol on APD_{80} and $CaTD_{80}$ in the whole left ventricle (LV) of sham and MI hearts. (A) APD_{80} and percent change in APD_{80} (B). (C) CaTD80 and percent change in $CaTD_{80}$ (D). Data are means ±SD, N= 3-5 hearts/group, *P<0.05, ***P<0.001, ****P<0.0001, by two-way ANOVA with repeated measures (A & C) or unpaired t-test (B & D)

Discussion:

Post-MI sympathetic hypo-innervation has been shown to be an indicator of ventricular arrhythmias and sudden cardiac death (Fallavollita et al. 2014). Previous work has shown that CSPGs block sympathetic nerve re-growth in the infarcted region (Ryan T. Gardner and Habecker 2013). Additionally, mice with regional sympathetic nerve loss have super-sensitive

responses to ß-AR agonists, increased APD dispersion, and increased risk for ventricular arrhythmias (Tapa et al. 2020; R. T. Gardner et al. 2015). Thus, the goal of this study was to determine the electrophysiological and sympathetic remodeling that occurs post-MI in a fully innervated rabbit heart preparation. In this study, we show that: (1) CSPGs are present in the hypo-innervated infarct region; (2) physiological sympathetic nerve stimulation produces an increase in APD dispersion and increased susceptibility for VT/VF in MI vs. sham hearts; and (3) despite significant hypo-innervation, MI hearts remain responsive to physiological nerve stimulation, potentially via preserved or slightly elevated ß-adrenergic responsiveness.

CSPGs and Sympathetic Nerve Remodeling post-MI:

Previous studies in mouse hearts have shown that CSPGs in the infarct region bind protein tyrosine phosphatase receptor sigma (PTPσ) present on sympathetic neurons to inhibit nerve re-growth post-MI (R. T. Gardner et al. 2015; Ryan T. Gardner and Habecker 2013). Additionally, genetic deletion or pharmacological inhibition of PTPσ allows for sympathetic reinnervation of the infarct (Blake et al. 2023; 2022b). In the present study, we found CSPGs present in both the infarct and border zone regions of post-MI rabbit hearts (Fig. 1A). Moreover, the infarct region had a significant reduction in sympathetic nerve density compared to remote regions (Fig. 1B). These results are in agreement with previous findings in which CSPGs, particularly sulfated CSPGs, were found to prevent sympathetic nerve re-growth (Blake et al. 2023; R. T. Gardner et al. 2015; Ryan T. Gardner and Habecker 2013). Although we did not assess sulfation of CSPGs in this study, we did find CSPGs to be associated with hypo-innervation, suggesting similar mechanisms in the rabbit compared to mouse model. Interestingly, CSPGs are not present in infarcts that are not reperfused (chronic ligation models) (Ryan T. Gardner and Habecker 2013).

Therefore, the cellular source of CSPGs and how CSPG expression is impacted by reperfusion remains an important area for future study.

Electrophysiological Remodeling post-MI:

With SNS, MI hearts had a gradual increase in APD dispersion compared to sham (Fig. 3C). These results are similar to previous studies in models of MI, as well as models of sympathetic denervation without MI, in which adrenergic stimulation with isoproterenol led to an increase in APD dispersion (Tapa et al. 2020; R. T. Gardner et al. 2015). Similarly, in patients with post-infarct cardiomyopathy, both direct ß- adrenergic stimulation (with isoproterenol infusion) and reflex sympathetic stimulation (with nitroprusside) resulted in a significant increase in ARI dispersion (a surrogate for APD) (Vaseghi et al. 2012b). The increased APD (or ARI) dispersion observed with both direct pharmacological ß- adrenergic stimulation and sympathetic nerve activation is likely a result of heterogeneous sympathetic innervation as well as heterogeneous changes to adrenergic sensitivity post-MI. It is known that increased heterogeneity of refractoriness or increased APD dispersion provides a substrate for unidirectional conduction block and reentry and is therefore pro-arrhythmic(Ripplinger et al. 2022). Accordingly, in the present study, we found that there was a trend for increased susceptibility to pacing-induced ventricular arrhythmias during SNS in post-MI hearts (Fig. 3E).

We also found that post-MI hearts had significantly shortened APD_{80} in the infarct region compared to baseline with SNS (Fig 4B – 4D). This result is interesting, as it suggests that the hypo-innervated myocardium is still sensitive and responsive to sympathetic nerve stimulation. These findings could be due to changes in the amount of NE released from the remaining

sympathetic nerves in the infarct region, changes in NE reuptake (which may result in increased NE diffusion from nearby nerves), or changes in the ß-adrenergic sensitivity of the myocardium. Indeed, previous work in denervated rodent hearts showed that hypo-innervated regions demonstrated ß-adrenergic supersensitivity (Tapa et al. 2020). To assess ß-adrenergic sensitivity in the present study, electrophysiological responses to ISO were assessed. We found that ISO resulted in significant shortening of APD_{80} and $CaTD_{80}$ from baseline values in MI hearts (5A & 5C); indicating that the myocardium was responsive to direct ß – adrenergic stimulation. Additionally, we found that MI hearts had a significantly greater relative shortening in $CaTD_{80}$, but not APD_{80}, compared to sham (Fig 5B & 5D). Taken together, these results suggest that at 9-11 days post-MI, rabbit hearts are at least as sensitive to direct stimulation of ß receptors compared to sham hearts, with perhaps slightly elevated sensitivity as indicated by the larger change in $CaTD_{80}$. It is possible that more overt supersensitivity may develop at later timepoints post-MI.

Conclusions:

Using the innervated rabbit heart model, we evaluated the electrophysiological and sympathetic remodeling that occurs 9-11 days post-MI. We found that CSPGs were present in the infarct region, and were associated with areas of sympathetic hypo-innervation. These findings suggest that the mechanisms of post-MI sympathetic remodeling may be similar in rodents and larger mammals, including humans. Moreover, hypo-innervated post-MI hearts remained responsive to both direct sympathetic nerve stimulation and pharmaceutical sympathetic nerve activation while demonstrating pro-arrhythmic responses to direct sympathetic nerve stimulation. Taking this into

account these findings could carry significant implications for post-MI cardiac function and susceptibility to arrhythmias.

Study Limitations:

In this study, due to the technical complexity of the ischemia-reperfusion surgery and challenges with the innervated rabbit heart preparation, we have a small sample size for some of the parameters assessed. Only a single post-MI timepoint was evaluated. Future studies that assess sympathetic and electrophysiological remodeling over a longer time course are warranted.

Chapter III: The Effect of Chronic Nicotine Exposure on Cardiac Electrophysiology in the Rabbit Heart

Abstract

Introduction: The objective of this study was to determine the effect of chronic nicotine exposure on sympathetic remodeling, cardiac electrophysiology, Ca^{2+} handling, and arrhythmia susceptibility in the rabbit heart.

Methods: Rabbits were exposed to nicotine (NIC) via a transdermal patch (21 mg/day, 28 days, N =11) or a control adhesive patch (CT, N =8). Fully innervated isolated hearts were optically mapped using voltage- (RH237) and calcium-sensitive (Rhod2-AM) indicators. Sympathetic nerve stimulation (SNS) was performed with electrical stimulation of the spinal cord at the 1st – 3rd thoracic vertebrae, in which voltage was kept constant (7 V) and frequency was increased in 0.5 Hz increments until a threshold of 15% increase in heart rate (HR) was achieved. ß-adrenergic (ß-AR) responsiveness was evaluated with norepinephrine (NE, 500nM). Sympathetic nerve density was assessed by immunohistochemistry for tyrosine hydroxylase (TH) and NE content was quantified by high performance liquid chromatography (HPLC).

Results: *Ex vivo* baseline HRs were significantly faster in NIC vs. CT (206.3 ± 24.5 BPM vs 166.6 ± 38.8 BPM, P=0.01) and SNS stimulation thresholds were significantly increased in NIC vs. CT (7.3 ± 5.3 Hz vs 2.1 ± 1.0 Hz, P=0.01). Action potential duration (APD) alternans emerged at longer pacing cycle lengths (PCL) in NIC vs. CT both at baseline (238.8 ± 15.5 ms

vs 197.5 ± 22.5 ms, P=0.002) and during SNS (230.0 ± 22.7 ms vs 180.0 ± 28.3 ms, P=0.0003), with similar results obtained for Ca^{2+} transient alternans. SNS significantly reduced the PCL at which alternans emerged in CT but not NIC. NIC hearts tended to have less of a relative change in HR from initial values after NE perfusion and took longer to reach a significant elevation in HR compared to CT. There was no significant difference in fibrosis density between NIC and CT. NIC hearts had significantly less TH+ area compared to CT (7.6 ± 0.9% vs 10.2 ± 2.5%,P=0.03) and a trend for higher NE content in the left ventricle and right atrium compared to CT.

Conclusions: These results suggest that chronic nicotine exposure results in higher *ex vivo* HRs and SNS thresholds, reduced sympathetic nerve density, increased susceptibility for APD and Ca^{2+} alternans, and altered ß-AR responsiveness. These results are likely due to both sympathetic hypo-innervation of the myocardium and diminished adrenergic responsiveness after nicotine exposure. Our data indicate that after 4 weeks of exposure, nicotine results in potentially detrimental sympathetic and electrophysiological remodeling.

Abbreviations:

NIC (nicotine-exposed hearts), AP (action potential), APD (action potential duration), APD_{80} (action potential duration at 80% repolarization), Ca^{2+} (calcium), CaT (calcium transient), CaTD (calcium transient duration), $CaTD_{80}$ (calcium transient duration at 80% repolarization), CT (control hearts), HR (heart rate), HRV (heart rate variability), LV (left ventricle), nAChR (nicotinic acetylcholine receptor), NE (norepinephrine), PCL (pacing cycle length), PVC

(premature ventricular contraction), SCD (sudden cardiac death), SHS (second hand smoke), SNS (sympathetic nerve stimulation)

Introduction

Cigarette smoking is the most preventable cause of cardiovascular illness and fatalities in the United States (He et al. 2022; Gallucci et al. 2020; Mensah and Brown 2007) . Additionally, smoking contributes significantly to the progression of coronary artery disease thereby increasing the risk for myocardial infarction (MI), heart failure (HF), ischemia-induced arrhythmias and sudden cardiac death (Aune et al. 2018; Deo et al. 2016; Barua and Ambrose 2013). It has been shown that short-term secondhand smoke (SHS) exposure increases the incidence for atrial fibrillation and ventricular tachycardiac/fibrillation (C.-Y. Chen et al. 2008). Previous work from our lab has shown that longer-term SHS exposure (4-12 weeks) increases the susceptibility to Ca^{2+} and action potential duration (APD) alternans, which may contribute to arrhythmias with SHS exposure (Z. Wang et al. 2018). However, which individual components of cigarette smoke may contribute to alternans and smoking-related arrhythmias are largely unknown. Recently, cigarette sales have declined but the prevalence for electronic cigarette (e-cigarette) usage has increased. In a recent study released by the Center for Disease Control and Prevention it was reported that e-cigarette unit sales increased by 46.6% between 2020 – 2022 (Ali 2023). In e-cigarettes there are many different components present; such as, tobacco-specific nitrosamines, aldehydes, and flavors to name a few (Lisko et al. 2015; Kim and Shin 2013; Lim and Shin 2013; Pellegrino et al. 2011). However, a common factor between smoking and vaping is nicotine exposure. The amount of nicotine present in e-cigarettes is often variable and in cases

has been reported to be higher than an entire pack of conventional cigarettes (Goniewicz et al. 2019; Pankow et al. 2017). Nicotine which has been associated with structural and electrophysiological remodeling of the myocardium and alterations in autonomic regulation that can be pro-arrhythmic.

Nicotine has been associated with increased myocardial fibrosis (Shan et al. 2009; Goette et al. 2007; Miyauchi et al. 2005), which may play a role in creating a heterogeneous substrate that can foster ectopic activity and/or reentrant arrhythmias (Kléber and Rudy 2004). In line with these findings, *in-vivo* administration of nicotine was reported to result in atrial and ventricular arrhythmias in a canine model of MI (Yashima et al. 2000; Mehta et al. 1997). Meta analysis studies on nicotine replacement therapies have found that there is an increased risk of rhythm disorders (Mills et al. 2014; 2010). However, there has been little mechanistic work done on the effect of *chronic* nicotine exposure on cardiac electrophysiological remodeling and arrhythmogenesis.

Nicotine is also associated with increased sympathetic activity. In particular, acute exposure to e-cigarettes containing nicotine has been linked to reduced heart rate variability (HRV) (Moheimani, Bhetraratana, Yin, et al. 2017), and in the clinical setting reduced HRV has been associated with increased sympathetic activity and risk for sudden cardiac death (SCD) (Shekha et al. 2005; Malliani et al. 1994). Thus, it is possible that long-term nicotine use results in autonomic dysregulation that may also play a role in promoting detrimental ventricular arrhythmias.

Nicotine can impact autonomic control of the heart because it binds nicotinic acetylcholine receptors (nAChR) that are present within the brain, the peripheral nervous system, and adrenal medulla (Grilli et al. 2005). In studies on rats using labeled norepinephrine, it was found that rats given nicotine for 10 days had a higher outflow of norepinephrine and lower outflow of acetylcholine than vehicle-treated rats in the hippocampus (Grilli et al. 2005), indicating that the overall net effect from the central nervous system is sympathetically driven and that chronic nicotine exposure could lead to sympathetic hyperactivity.

Nicotine acts on the peripheral nervous system by binding to nAChRs present on the post ganglionic neurons of the parasympathetic and sympathetic nerves innervating the heart (Grilli et al. 2005), which under certain circumstances could lead to autonomic imbalance. Additionally, there are nAChRs present on cardiomyocytes. Previous findings have indicated that α7 nAChR to be present on adult ventricular cardiomyocytes (Dvorakova et al. 2005) indicating that nicotine can act directly on cardiomyocytes. As such, work in isolated cardiomyocytes using nicotinic receptor antagonists has shown that acute nicotine administration directly blocks the membrane stabilizing current I_{k1} (H. Wang, Yang, et al. 2000; H. Wang, Shi, et al. 2000). We have previously shown that I_{k1} blockage leads to ectopic beats (Myles et al. 2015). Therefore, nicotine targets the central nervous system, autonomic nervous system, and cardiomyocytes such that the contribution of these effects may produce detrimental cardiac effects and arrhythmias. Currently, there has been little research done on the effect of *chronic* nicotine exposure on calcium handling and cardiac electrophysiological remodeling. Therefore, the goal of this study

was to investigate the interaction between chronic nicotine exposure and Ca^{2+} handling, arrhythmia susceptibility, structural remodeling, and sympathetic remodeling.

Methods

Ethical Approval

All procedures were approved by the Animal Care and Use Committee of the University of California, Davis and were conducted according to the Guide for the Care and Use of Laboratory Animals published by the National Institutes of Health. Male and female New Zealand White rabbits (NZW) were obtained from Charles River with a delivery weight of 3.0 – 3.5 kg and were singly housed with *ad libitum* access to food and water for the duration of the exposure. Rabbits were 4 – 8 months of age at time of study. A total of N=25 rabbits (10 male, 15 female) were studied and exposure was carried out in 4 sequential cohorts with approximately matched numbers of control and nicotine exposure in each cohort. Due to the limited success of sequential *in vivo* blood collection and some *ex vivo* experimental procedures, sample sizes and sex distribution are unequal for some parameters. Likewise, in some cases the *ex vivo* innervated heart preparations did not capture at a particular pacing frequency, which impacted sample size for some rate-matched parameters. All n-numbers are detailed within each figure legend with symbols indicating sex.

Nicotine Exposure

Rabbits were exposed to nicotine (NIC) via transdermal patch (Nicoderm CQ, 25mg/day) placed on the ears. Transdermal patches were changed daily Monday – Friday for 4 weeks. Control

(CT) rabbits had surgical tape placed on the ears and were handled daily in the same manner as NIC rabbits. Venous blood draws were performed on rabbits the day prior to the start of exposure, at 2 weeks, and at 4 weeks after the start of exposure on both NIC and CT rabbits via the marginal ear vein. Blood samples were allowed to clot overnight at 2 – 8 C. Then centrifuged at 1000 x g (or 3000 rpm) for 15 minutes. Serum was removed and then stored at -80°C. To assess serum cotinine levels, samples were sent overnight on dry ice to the Tobacco and Carcinogen Biomarkers Core at the University of California San Francisco and were analyzed by liquid chromatography-tandem mass spectrometry (LCMSM) as previously described(Jacob et al. 2011).

Innervated Whole-Heart Langendorff Perfusion

At 28 days of exposure, rabbits were weighed and given a single intravenous injection of pentobarbital sodium (50mg/kg) containing 1000 IU heparin (Fresenius Kabi USA, IL). Isolated innervated rabbit hearts were surgically extracted with an intact thoracic spinal column (T1 – T12) as in previous studies (L. Wang et al. 2019; Ng, Brack, and Coote 2001b). Following extraction, the isolated preparation was flushed with ice cold cardioplegia (composition in mmol/L: NaCl 110, $CaCl_2$ 1.2, KCl 16, $MgCl_2$ 16, and $NaHCO_3$ 10) via the descending aorta. The preparation with intact spinal cord and heart was then retrograde perfused with Tyrode's solution at 37± 0.5° C (composition in mmol/L: NaCl 128.2, $CaCl_2$ 1.3, KCl 4.7, $MgCl_2$ 1.05, NaH_2 PO4 1.19, $NaHCO_3$ 20 and glucose 11.1). The preparation was then submerged in warm Tyrode's and perfused with an excitation-contraction uncoupler (blebbistatin, 10 – 20 uM, R&D Systems INC, Minneapolis, MN, USA) and a skeletal muscle paralytic (vecuronium bromide, 6 uM, Cayman Chemical Company INC, Ann Arbor, MI, USA) to eliminate motion during optical

recordings. Two needle electrodes were positioned in the thoracic cavity and a ground was placed in the bottom of the perfusion dish to obtain a continuous ECG recording. Perfusion pressure was maintained at 60 – 80mmHg by adjusting perfusion flow rate (80 – 100mL/min).

Optical Mapping

Dual optical mapping was performed as in previous studies(L. Wang et al. 2019; Francis Stuart et al. 2018, 2; Myles et al. 2012). Briefly, preparations were loaded with calcium-sensitive dye (Ca2+; Rhod 2 – AM, 50uL of 1mg/mL in DMSO + 10% pluronic acid, Biotium, Hayward, CA) and voltage-sensitive dye (Vm; RH237, 50uL of 1mg/mL in DMSO, Biotium, Hayward, CA) through the coronary perfusion. A catheter electrode was inserted up the spinal canal to T1 -T3 in order to stimulate the pre-ganglionic sympathetic nerves. A pacing electrode was placed on the center of the left ventricle for epicardial ventricular pacing. The anterior epicardial surface was illuminated with LED light sources at 530 nm bandpass filtered from 511 to 551 nm (LEX-2, SciMedia, Costa Mesa, CA, USA) and focused directly on the surface of the heart. Florescence emitted was captured utilizing a THT-macroscope (SciMedia) and divided by a dichroic mirror set at 630 nm (Omega, Brattleboro, VT, USA). RH237 signals were long pass filtered at 700 nm, while Rhod2-AM signals were bandpass filtered from 574 to 606 nm. Signals were recorded with two CMOS cameras (MiCam Ultima-L, SciMedia). Data was recorded at a sampling rate of 1 kHz and a 100 x 100 pixel resolution, with a field of view of 3.1 x 3.1cm and a spatial resolution of 0.31mm/pixel.

Experimental Protocol

Prior to the addition of dyes and blebbistatin, *ex vivo* baseline heart rate (HR) was recorded via a continuous ECG recording. After the addition of blebbistatin, sympathetic nerve stimulation (SNS) thresholds were determined as previously described (Francis Stuart et al. 2018). Specifically, sympathetic nerve fibers were initially stimulated at 0.5Hz, 7V for 5 seconds. Stimulation frequency was then increased in 0.5Hz increments at a constant voltage of 7V until a >15% increase in HR was observed. Sympathetic nerve stimulation thresholds were then recorded, and for all subsequent optical imaging protocols, hearts were stimulated at 5Hz higher than their threshold value. SNS was performed for 13s to record baseline $Ca^{2+,}$ Vm, and HR values. Continuous ventricular pacing was then performed via the epicardial left ventricle (LV) at decreasing pacing cycle lengths (PCL) from 300ms until hearts lost capture. Finally, hearts were challenged with norepinephrine (NE, 500 nM) to evaluate ß adrenergic responsiveness.

Optical Mapping Data Analysis

Optical data was analyzed using both *Optiq* (Cairn Research Ltd, UK) and ElectroMap (O'Shea et al. 2019) and as described in our previous studies (Caldwell et al. 2023; Tapa et al. 2020; L. Wang et al. 2019). Briefly, action potential duration (APD_{80}) or Ca^{2+} transient duration ($CaTD_{80}$) was calculated as 80% repolarization minus activation time (with activation time calculated at 50% of peak amplitude). Mean APD_{80} and $CaTD_{80}$ for each heart were calculated from the entire mapping field of view. CaTD and APD alternans thresholds were determined using spectral methods as previously described (L. Wang et al. 2021; 2014). APD and CaTD alternans thresholds were defined as the slowest PCL for which significant alternans emerge (minimum spectral magnitude ≥2).

Data pertaining to changes in heart rate during SNS were analyzed from optical recordings using ElectroMap (due to SNS electrical artifacts on the ECG). All other HR measurements were obtained from continuous ECG recordings and analyzed using LabChart (ADInstruments INC, Colorado Springs, CO, USA). *Ex vivo* baseline HR was measured 1 minute prior to the addition of blebbistatin and averaged over 1 minute. For HR changes in response to NE, HR was measured 1 minute prior to the addition of NE (averaged over 10s) and 6 minutes after NE perfusion. Arrhythmia scores were analyzed during sinus rhythm according to previous studies(Francis Stuart et al. 2018; De Jesus et al. 2017; CURTIS and WALKER 1988). Briefly, 0 = no ectopic beats, 1 = premature ventricular contraction (PVC), 2 = bigeminy or salvos (2 – 4 consecutive beats), 3 = ventricular tachycardia (>5 consecutive, monomorphic beats), or 4 = ventricular fibrillation (>5 consecutive, polymorphic beats). Arrhythmia scores were determined as the most severe arrhythmia observed during the entire experimental protocol.

Immunohistochemistry and Histology

After optical mapping experiments, a 2 mm thick short-axis section was cut from the middle of the LV. The section was then cut into wedges such that samples from the same LV were used for HPLC analysis and immunohistochemistry. Tissue was fixed in 4% paraformaldehyde for 1.5 hrs, washed with phosphate buffered saline (PBS), and placed in 30% sucrose in PBS overnight. Tissue was then embedded in Optimal Cutting Temperature (OCT) medium, flash frozen, and stored at -80°C. Tissue sectioning and Masson's Trichrome staining was performed by Acepix Biosciences Inc (Hayward, CA, USA). Tissue was sectioned into 10 um thickness slices at a step depth of 50 – 100 um, thaw-mounted on positively charged slides, and stored at – 80°C.

Tyrosine hydroxylase (TH) labeling was performed as in previous studies(Tapa et al. 2020; Francis Stuart et al. 2018; Ryan T. Gardner and Habecker 2013). Briefly, slides (N = 6 slices/group) were rehydrated with PBS and incubated in sodium borohydride (10mg/mL) in order to reduce background auto-florescence. Slides were then blocked with 2% bovine serum albumin (BSA, Sigma) and 0.3% Triton X-100 (Sigma) in PBS (BSA/PBST) for 1 hr. Slides were then washed in PBS and incubated primary sheep anti-TH (EMD Millipore) at 1:300 BSA/PBS-T overnight at room temperature. Slides were then rinsed in PBS and incubated in secondary antibody (1:500; Invitrogen) for 1.5 hr at room temperature. After incubation, slides were rinsed with PBS, dipped in MilliQ water briefly and then incubated in a 10 mM copper sulfate/50 mM ammonium acetate solution to reduce autofluorescence. Finally, slides were dipped in MilliQ water briefly and a 1:1 glycerol/PBS solution was used to coverslip.

Histological and fluorescence imaging was performed on an upright Nikon Eclipse Ni microscope at 10x magnification with a FITC filter (Ex/Em: 495/519 nm) for TH, and at 20x magnification with white light excitation for Masson's trichrome. For TH, four images per tissue slice were taken and ImageJ was used to threshold TH+ sympathetic nerve fiber area and total tissue area. Percent fiber density was defined as the ratio of TH+ fiber area to total tissue area. For Masson's trichrome staining, fibrosis area was color-thresholded (blue) and divided by total tissue area. All images were analyzed by two blinded users and values averaged between users.

Tissue Norepinephrine Content

Norepinephrine (NE) content was measured via HPLC as described previously (Francis Stuart et al. 2018; Parrish et al. 2010). After optical mapping, LV and right atrial samples were flash frozen and stored at -80°C. Tissue was then homogenized at 25°C in perchloric acid (PCA, 0.1 M) and an internal standard—dihydroxybenzylamine (DHBA, 0.25 uM) to correct for NE sample recovery. Catecholamines were purified from a 100 uL aliquot of homogenate using alumina extraction. NE was reabsorbed from alumina by using PCA (150 uL, 0.1 M) and then measured by C18 reversed-phase HPLC with electrochemical detection (ESA, Coulchem III) and a detection limit of ~ 0.05 pmol and > 60% recovery from alumina extraction.

Statistics

Data are expressed as mean ± standard deviation (SD). Two-tailed, unpaired *t*-test was used to assess differences between NIC and CT for the following parameters: baseline HR, SNS threshold, percent change in HR, $CaTD_{80}$, and APD_{80}, arrhythmia scores, and maximum HR after NE. T-tests were performed on fibrosis density and TH+ fiber density. Two–way ANOVA with repeated measures was used to assess data obtained at baseline and in response to SNS or NE within the same heart. Two-way ANOVA with mixed-effects analysis was used on HR changes in response to NE and NE content. Statistics were performed using GraphPad Prism 9. Statistical significance was defined by $P<0.05$.

Results:

Baseline Measurements Following Nicotine Administration:

To confirm nicotine delivery, cotinine (main metabolite of nicotine) was measured in serum blood samples. As expected, CT rabbits had no detectable cotinine present in blood serum for all time points (Fig 6A). In NIC rabbits, there was no detectable cotinine present at time 0, and cotinine concentration increased to 455.3 ± 374.0 ng/mL and 694.6 ± 376.4 ng/mL at 2 and 4 weeks, respectively. To determine the impact of nicotine on *ex vivo* HR*;* baseline HR measurements were obtained from the innervated perfused heart preparations prior to the addition of blebbistatin and dyes. NIC hearts had significantly faster HRs compared to CT (Fig 6B, 206.3 ± 24.5 BPM vs 166.6 ± 38.8 BPM). SNS stimulation thresholds were also increased in NIC hearts (Fig 6C, 7.3 ± 5.3 Hz vs 2.1 ± 1.0 Hz).

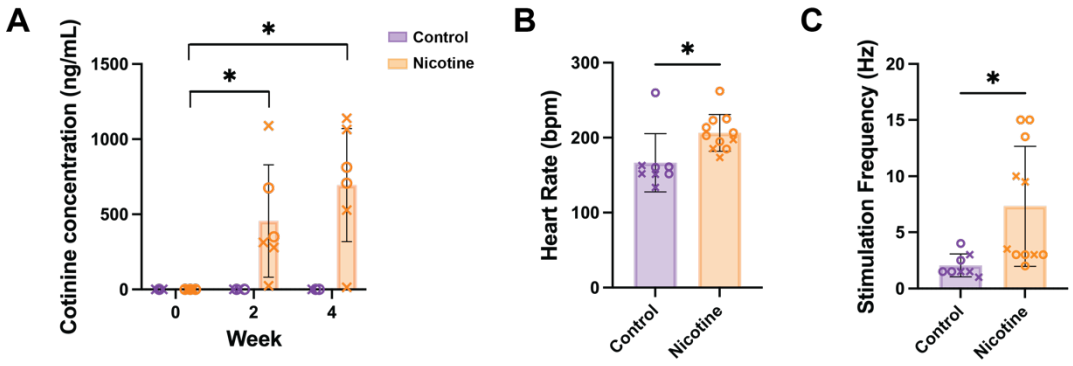

Figure 6: Cotinine concentration, heart rate, and sympathetic nerve stimulation threshold in control and nicotine-exposed hearts. (A) Mean cotinine concentration at 0, 2, and 4 weeks of nicotine exposure. *P<0.05, N= 6 - 10 animals/group, by two-way analysis of variance (ANOVA). (B) Ex vivo baseline heart rate. Measurements taken prior to the addition of dyes and blebbistatin. *P<0.05, N= 8-11 hearts/group. (C) Stimulation frequency threshold for sympathetic nerve stimulation (SNS). Spinal cord was stimulated at T1 - T2

with constant voltage and frequency was increased 0.5Hz increments until a >15% increase in heart rate was observed. *P<0.05, N= 8-11 hearts/group, by two- tailed unpaired t test. X denotes males, O denotes females

Electrophysiological Responses to Sympathetic Nerve Stimulation (SNS):

To determine the effect of SNS on electrophysiological parameters, APD_{80}, $CaTD_{80}$, and HR, were measured immediately prior to and at 13s of SNS. SNS significantly shortened APD_{80} to a similar degree in both CT and NIC hearts (Fig 7A-B). SNS caused significant shortening of $CaTD_{80}$ compared to baseline values in CT but not NIC hearts (Fig 7C), but the mean percent change in $CaTD_{80}$ with SNS was not different between groups (Fig 7D, -11.6 ± 12.5% vs. -7.2 ± 10.3%). Similar to HR data obtained prior to the addition of dyes and blebbistatin (Fig 7B), baseline HR remained slightly faster in NIC hearts compared to CT (Fig 7E, 152.4 ± 14.5 BPM vs. 134.4 ± 17.1 BPM, P = 0.62). However, both groups had similar increases in HR with SNS (Fig 7E-F, 196.8 ± 49.7 vs. 191.9 ± 72.5 BPM).

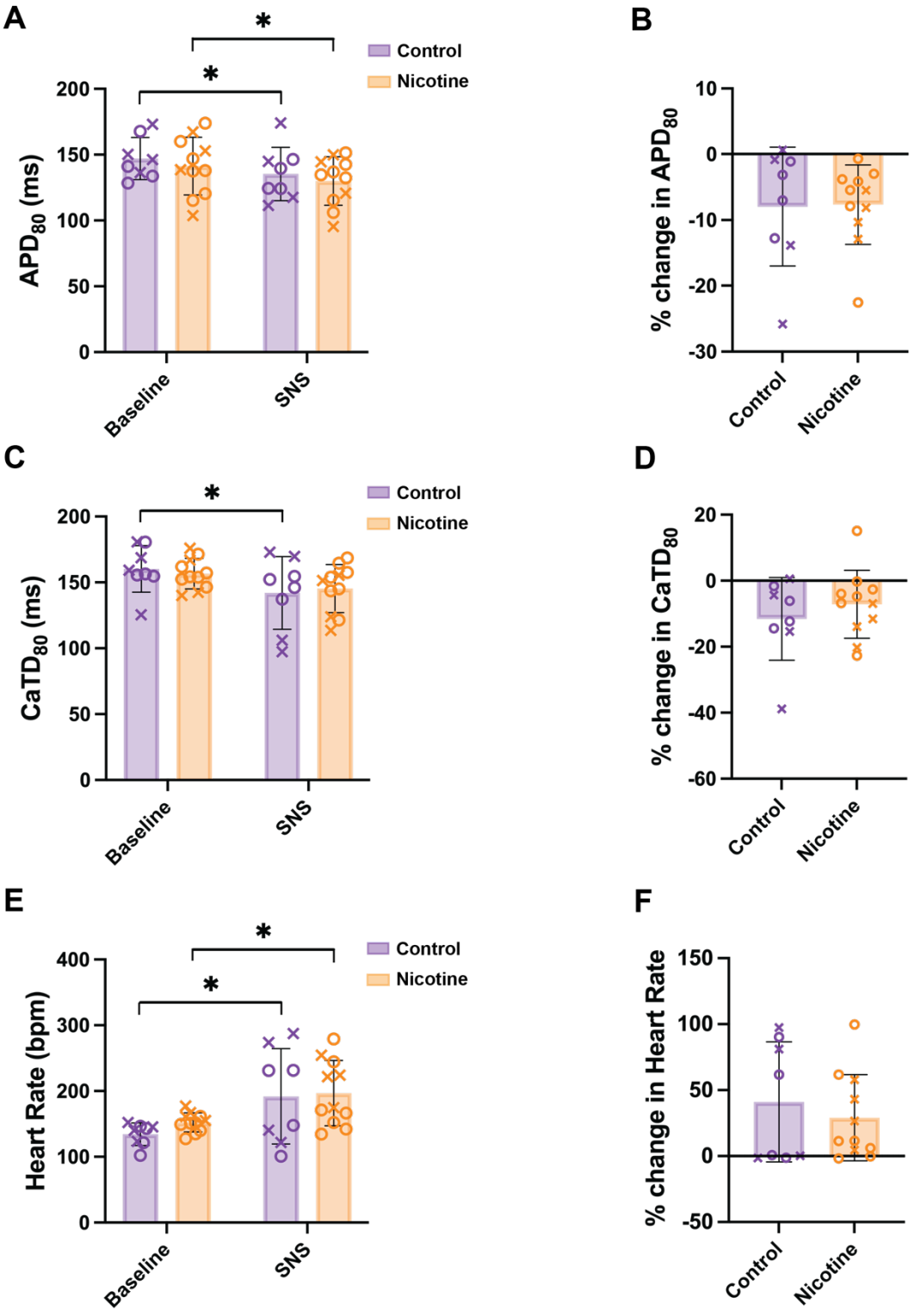

Figure 7: Effect of sympathetic nerve stimulation (SNS) on control and nicotine-exposed hearts. (A - B) Action potential duration (APD_{80}) changes with SNS. (C - D) Calcium transient

duration ($CaTD_{80}$) changes with SNS. (E - F) Heart rate changes with SNS. Data are means ± SD; N = 8-11; *P<0.05, by two-way ANOVA with repeated measures (A, C, E) or two-tailed, unpaired t test (B, D,F)

APD and CaTD Alternans:

In order to evaluate alternans susceptibility, hearts were paced at progressively faster pacing cycle lengths (PCLs). Hearts were initially paced at baseline and then at the same PCL with SNS. At baseline, APD alternans emerged at significantly longer PCLs in NIC compared to CT hearts (Fig 8A, 238.8 ± 15.5 ms vs 197.5 ± 22.5 ms) and similarly with SNS (230.0 ± 22.7 ms vs 180.0 ± 28.3 ms). Sympathetic stimulation may decrease alternans PCL threshold due to accelerated Ca^{2+} handling (L. Wang et al. 2019; Tomek et al. 2017). Surprisingly, NIC hearts had no significant difference between baseline and SNS APD alternans thresholds; however, SNS significantly decreased alternans PCL threshold in CT hearts as expected. Similar results were obtained for CaTD alternans (Fig 8B). Figure 3C-D show representative contour maps of CaTD alternans spectral magnitude and example optical traces at baseline and with SNS showing little-to-no change in CaTD alternans with SNS in NIC hearts (Fig 8D).

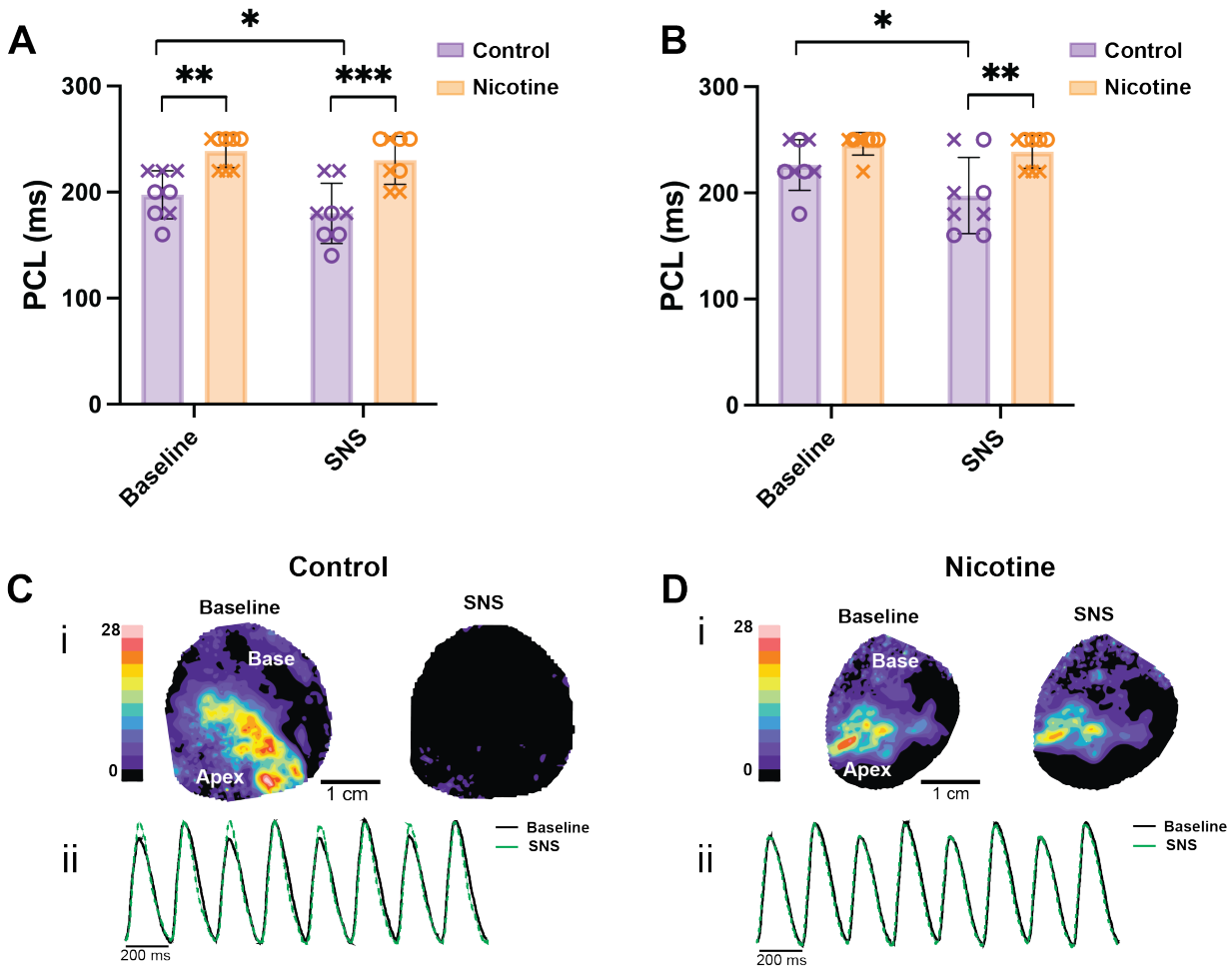

Figure 8: Alternan threshold and magnitude with SNS in control and nicotine-exposed hearts. (A) Pacing cycle length (PCL) at which APD alternans emerged at baseline and with SNS. (B) PCL at which Ca2+ alternans emerged (C) and (D), representative contour maps and corresponding CaTD traces demonstrating Ca2+ alternan magnitude at baseline and with SNS (C, control; D, nicotine). Data are means ± SD; N = 8/group; *P<0.05, **P<0.01, ***P<0.001, by two-way ANOVA with repeated measures.

β-Adrenergic Responsiveness:

Electrophysiological differences in response to SNS may be due to altered nerve function (e.g., NE release), altered β-adrenergic responses of cardiomyocytes, or a combination of both; therefore, norepinephrine (NE) was added the perfusate to specifically assess β-adrenergic responses of cardiomyocytes. HR prior to the addition of NE (time 0, t0) up to 6 minutes after the addition of NE is shown in Fig 9A. To account for differences in baseline HR, the percent change in HR over 6 minutes of NE perfusion was also calculated (Fig 9B). CT hearts tended to have a larger relative change in HR from initial values at all time points compared to NIC, but this was not statistically significant. Both groups had significantly faster HRs at 2 and 3 min after NE compared to t0 (Fig 9C), but only CT hearts showed significant elevation at 1 min, suggesting a potentially slower HR response in NIC hearts. Maximal HRs after the addition of NE were not significantly different between groups (CT: 216.4 ± 51.4 BPM vs. NIC: 205.2 ± 45.5 BPM).

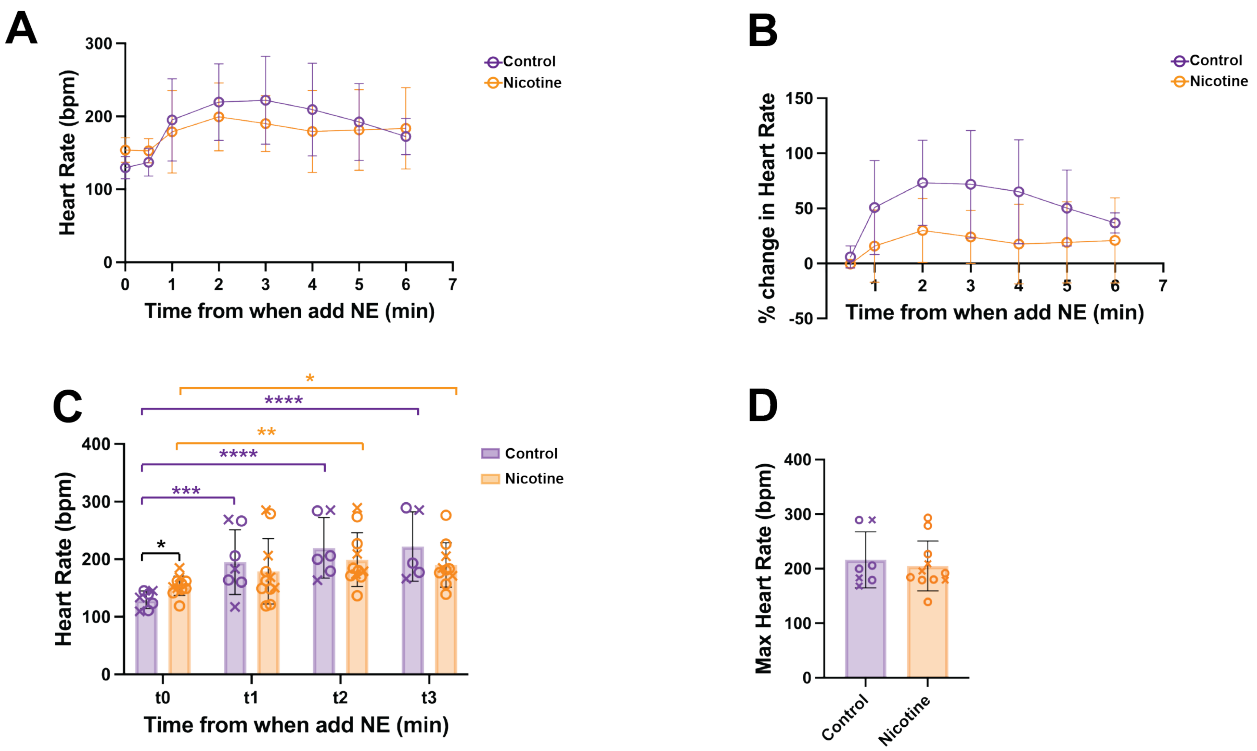

Figure 9: Heart rate changes with Norepinephrine in control and nicotine-exposed hearts (A - B) Heart rate changes over time after the addition of 500nM Norepinephrine (NE) to the perfusate. N = 7 - 11/group (C) Heart rate measurements after the addition of NE at 1 minute (t1, N = 7 -11/group), 2 minutes (t2, N = 6 - 11/group), and 3 minutes (t3, N = 5 - 10/group). (D) Maximum heart rate after NE added, N = 7 -11/group *P<0.05, **P< 0.01, ***P<0.001, ****P<0.0001, by two-way ANOVA with mixed-effects analysis (A - B) or two-tailed, unpaired t test (D)

Arrhythmia Susceptibility:

Arrhythmia susceptibility was measured from bipolar ECG recordings taken from needle electrodes inserted into the posterior thoracic cavity (hence atypical ECG morphology). Hearts from both groups had PVCs and bigeminy/salvos, but there were no significant differences in arrhythmia score between CT and NIC hearts (Fig. 10, CT: 0.88 ± 0.83 vs. NIC: 1.5 ± 0.71).

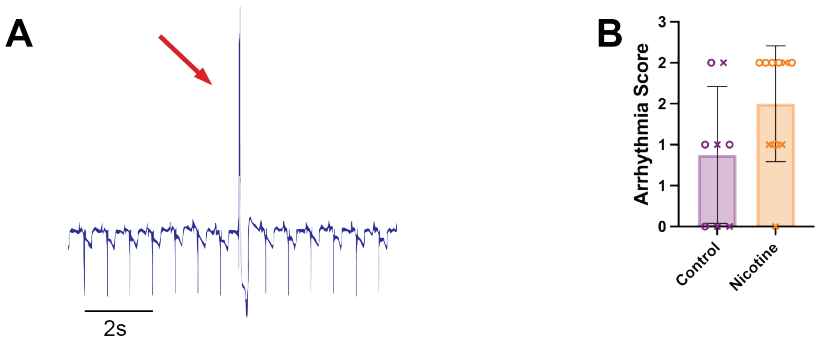

Figure 10: Arrhythmia susceptibility in control and nicotine-exposed hearts. Psuedo - ECG recordings demonstrating arrhythmias during sinus rhythm or following rapid ventricular pacing. Recordings were measured from the posterior in the bath. (A) example of a pre-ventricular contraction (PVC) denoted by the red arrow (B) Average arrhythmia scores per group. Data are means ± SD, N= 8 - 10, by two-tailed, unpaired t test

Fibrosis, Sympathetic Nerve Density, and Norepinephrine Content:

Chronic nicotine administration has been previously associated with increased myocardial fibrosis (Miyauchi et al. 2005; Shan et al. 2009; Goette et al. 2007). Therefore, fibrotic density was evaluated from Masson's trichrome images. There was no significant difference in fibrosis density between CT hearts and NIC hearts (Fig 11A-B, 21.78 ± 3.68% vs. 19.30 ± 3.68%). To assess whether changes in sympathetic nerve density were responsible for altered SNS responses, the percent TH+ fiber density was quantified from LV tissue. CT hearts had a significantly higher percent area that was TH+ compared to NIC hearts (Fig 11C-D, 10.18 ± 2.45 % vs. 7.55 ± 0.91%). NE content was also measured in the left ventricle and right atria. As expected, there was a main effect of location, with the right atrium having higher NE content compared to the LV (due to greater sympathetic nerve density in the atrium versus ventricle). This was statistically significant in the NIC but not CT group (Fig 11E). Interestingly, despite the lower

ventricular nerve density, NIC hearts had a trend for higher NE content in the left ventricle compared to CT (29.2 ± 9.5 pmol/mg vs. 25.6 ± 8.4 pmol/mg) with a similar trend in the right atria (44.6 ± 12.1 pmol/mg vs. 34.8 ± 9.3 pmol/mg).

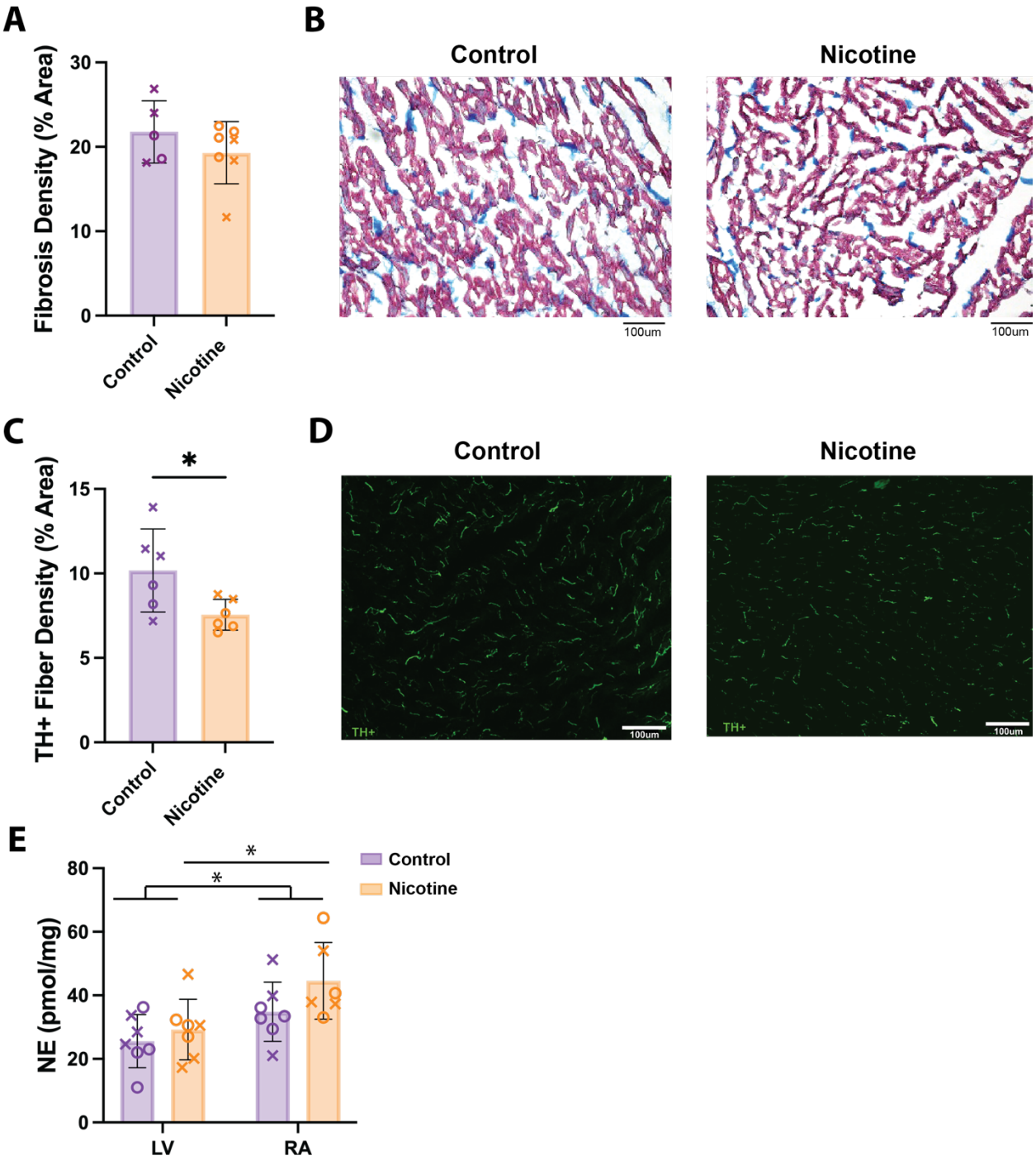

Figure 11: Fibrosis, sympathetic nerve density, and norepinephrine content in control and nicotine-exposed hearts (A) Average fibrosis density in left ventricle. N = 5 – 7 slides/group (B) Representative images of Masson's Trichrome staining; fibrosis indicated in blue and myocardial tissue in red (C) Sympathetic nerve fiber density in left

ventricle. N = 6 slices/group (D) Representative immunofluorescence images of tyrosine hydroxylase (TH) labeling. (E) Norepinephrine (NE) content of left ventricle (LV) and right atria (RA) N = 7 hearts/group. Data are means ±SD; *P<0.05 by two-tailed, unpaired t test (A & C) or two-way ANOVA with repeated measures (E). Scale bar = 100 μm

Discussion:

The objective of this study was to investigate the effects of chronic nicotine exposure on cardiac sympathetic responses, electrophysiological and structural remodeling, and potential arrhythmogenic effects. To our knowledge, this study is the first to employ the innervated rabbit heart model to evaluate sympathetic responses in hearts chronically exposed to nicotine. Here, we show that nicotine-exposed hearts had: (1) higher *ex vivo* baseline HRs; (2) elevated SNS thresholds and reduced sympathetic nerve density; (3) increased susceptibility to Ca^{2+} and APD alternans that does not improve with SNS; (4) altered ß-adrenergic responsiveness; and (5) no change in arrhythmia propensity. Taken together, these results suggest that chronic nicotine exposure leads to sympathetic remodeling and altered cardiac electrophysiological responses, but that these changes are not necessarily arrhythmogenic following 28 days of exposure.

Chronic Nicotine Exposure Increases Ex Vivo Baseline Heart Rate:

In isolated rabbit hearts it has been shown that perfusion of a low dose nicotine results in an acute increase in HR (Wennmalm 1977). Additionally, it has been shown that chronic nicotine administration leads to a reduction in heart rate variability (HRV) that suggests a shift to

sympathetic dominance and decreased vagal tone (Moheimani, Bhetraratana, Yin, et al. 2017; Moheimani, Bhetraratana, Peters, et al. 2017). Here, we show that the hearts of rabbits exposed to nicotine for 28 days have a sustained elevation in baseline *ex vivo* HR in the innervated heart preparation (Fig. 6B). Since the sympathetic innervation to the heart remains intact, this result may suggest an elevation in basal sympathetic nerve activity under resting conditions (without electrical stimulation) following nicotine exposure. Conversely, the increase in baseline HR may be due to functional and structural alterations within the SA node itself, which may represent an important area for future study.

Electrophysiological Responses to SNS After Chronic Nicotine Exposure

In this study, we found that hearts from nicotine-exposed animals had significantly increased electrical SNS thresholds (measured by the stimulation frequency required to produce a 15% increase in HR, Fig 7C). However, when nicotine-exposed hearts were stimulated with supra-threshold frequency, similar changes in APD, CaTD, and HR were observed (Fig 7). The elevated SNS thresholds could be due to many factors, including changes in sympathetic nerve density or function, altered b-adrenergic responsiveness, or structural remodeling of the myocardium. Chronic nicotine administration has been previously associated with increased myocardial fibrosis (Shan et al. 2009; Goette et al. 2007; Miyauchi et al. 2005); however, we found no significant difference in fibrosis in NIC compared to CT (Fig 11A). Sympathetic nerve loss after chronic nicotine exposure could also explain the blunted responsiveness to SNS, and as such, we found a reduction in sympathetic nerve density in NIC hearts (Fig 11C). Despite a decrease in nerve density, we observed a trend for elevated NE content in the right atrium and left ventricle of NIC hearts compared to CT (Fig 11E). Typically, NE content is associated with

local sympathetic nerve density (more nerves = more NE). However, this interesting result is similar to human and isolated rabbit heart studies that have shown that acute nicotine administration leads to an increase in NE release (Gourlay and Benowitz 1997; Gillespie et al. 1985; Löffelholz 1970). Additionally, findings in rats given chronic administration of nicotine have shown an increase in cardiac norepinephrine turnover rate (Westfall 1970).

Chronic Nicotine Exposure Increases the Susceptibility for APD and CaT Alternans

We found that NIC hearts had APD and CaT alternans that emerged at slower pacing cycle lengths compared to CTL (Fig 8A & 8B), indicating increased alternans susceptibility. This result is corroborated by previous work in post-MI dogs that showed an increase in depolarizing and repolarizing alternans after nicotine infusion (Yashima et al. 2000). Additionally, our previous study has shown a significant increase in the magnitude of APD and CaT alternans after second hand smoke exposure (Z. Wang et al. 2018). In normal hearts, b-adrenergic stimulation typically improves APD and CaT alternans due to acceleration of Ca^{2+} handling; thus it is expected that the PCL at which alternans emerge would decrease with SNS (L. Wang and Ripplinger 2019; Tomek et al. 2017). Indeed, SNS decreased the alternans threshold PCL in CTL hearts, but we found that SNS did not improve alternans thresholds in NIC hearts (Fig 8A & 8B). This result could be explained by decreased sympathetic responsiveness (potentially due to diminished sympathetic innervation) that may be particularly evident at faster PCLs. It is known that AP and Ca alternans are strongly associated with increased risk for ventricular arrhythmias (L. Wang et al. 2014; Laurita and Rosenbaum 2008; Chudin et al. 1999); however, we did not observe a statistically significant increase in arrhythmia susceptibility in NIC hearts in this study.

It is possible that increased arrhythmogenic activity may be observed with longer nicotine exposure.

ß-Adrenergic Responsiveness to NE after Chronic Nicotine Exposure

Because SNS may result in variable NE release (due to variations in nerve density and function), NE was directly added to the perfusate to assess ß-adrenergic responsiveness of the myocardium. NIC hearts tended to have somewhat smaller and slower changes in HR compared to CT (Fig 9). This may be a result of elevated HR in NIC hearts at time 0 (therefore any HR increases may be more modest),but could also suggest a somewhat blunted ß- adrenergic response. This blunted ß-adrenergic response could be due to ß- adrenergic receptor down regulation and as such twin studies on habitual smokers have shown a decreased ß- adrenergic receptor density and blunted catecholamine response compared to non-smokers (Laustiola et al. 1988). However, in this study we focused on changes in functional parameters as a result of chronic nicotine exposure and future studies would need to be performed in order to further elucidate these findings.

Conclusions:

Using the innervated rabbit heart model, we determined the effects of chronic nicotine exposure on cardiac electrophysiology, Ca^{2+} handling, and sympathetic remodeling and responses. We found that chronic nicotine exposure results in significantly reduced response to SNS, as indicated by significantly elevated electrical stimulation thresholds. Following nicotine exposure, SNS also failed to improve cardiac alternans, which may be pro-arrhythmic. These results are likely due to a combination of sympathetic hypo-innervation of the myocardium and diminished adrenergic responsiveness following nicotine exposure. Taken together, our data indicate that

chronic nicotine exposure results in potentially detrimental sympathetic and electrophysiological remodeling following 28 days of exposure.

Study Limitations:

In this study, we exposed rabbits to nicotine for 4 weeks and saw a change in some electrophysiological parameters of the heart but not all. It is possible that with longer exposure duration, there may be more profound changes in electrophysiology, calcium handling, and arrhythmia susceptibility. We specifically focused on ventricular action potentials, calcium transients, and nerve density in this study and therefore did not assess corresponding atrial parameters. Due to the technical challenges with the innervated rabbit heart preparation, we were insufficiently powered to assess sex differences in the context of chronic nicotine exposure, and this remains an important area for future study.

Chapter IV: Conclusions, Significance, and Future Directions

Summary of Main Conclusions:

The goal of this dissertation was to determine the effect of myocardial infarction and chronic nicotine exposure on sympathetic remodeling and activity in the rabbit heart. We evaluated cardiac electrophysiological remodeling in the context of action potential and calcium handling parameters, ß-adrenergic responsiveness, sympathetic nerve density, and structural remodeling. We found that both myocardial infarction and chronic nicotine exposure alter the response of the myocardium to physiological sympathetic nerve stimulation as well as direct pharmacological ß-adrenergic stimulation, resulting in pro-arrhythmic changes.

Sympathetic Responsiveness and Myocardial Infarction:

The key points in our myocardial infarction study are that chondroitin sulfate proteoglycans (CSPGs) were present in the sympathetic hypo-innervated infarct region. This is the first time the presence of CSPGs has been confirmed in a non-rodent model and the results suggest that post-MI sympathetic remodeling may be similar amongst rodents and larger mammals. With physiological sympathetic nerve stimulation (SNS), MI hearts had an increase in action potential duration (APD) dispersion and were more susceptible to detrimental arrhythmias. Additionally, we saw that despite significant hypo-innervation, post-MI hearts were responsive to physiological SNS, as indicated by significant shortening of APD_{80} in the infarct region. We also found that MI hearts were responsive to direct ß-adrenergic stimulation by Isoproterenol (ISO), as indicated by significant shortening of APD_{80} and $CaTD_{80}$ from baseline values. Moreover, MI

hearts had a greater relative shortening of $CaTD_{80}$ after ISO compared to sham. These findings indicate that at 9-11 days post-MI, rabbit hearts are at least as sensitive to direct ß-adrenergic stimulation vs. Sham, with potentially slightly elevated adrenergic sensitivity which may play a role in maintaining electrophysiological responses to nerve stimulation.

There are a number of differences and similarities between our MI and chronic nicotine exposure models. In our MI study there was an increased susceptibility for VT/VF; however, we did not see an increase in arrhythmia susceptibility in nicotine hearts. We did however see an increase in alternan susceptibility after chronic nicotine exposure which could lead to potentially detrimental ventricular arrhythmias with longer exposure times. Moreover, in our ischemia-reperfusion model there was an increase in fibrosis that we did not see after 4 weeks of nicotine exposure. This difference in fibrosis density could explain the differences in arrhythmia susceptibility between MI and nicotine hearts. Increased myocardial fibrosis is associated with increased susceptibility for arrhythmias because the heterogeneous substrate can foster ectopic and/or reentrant arrhythmias (Kazbanov, ten Tusscher, and Panfilov 2016; Kléber and Rudy 2004). Thus, it is possible that nicotine hearts had a lower risk for arrhythmias because they did not have an increase in fibrosis density after 28 days of exposure. Additionally, both models had differences in their responsiveness to direct ß-adrenergic stimulation. MI hearts had potentially an elevated ß-adrenergic sensitivity to isoproterenol; whereas, nicotine had a reduced sensitivity. These differences could be explained by differences in readout after perfusion of agonists (heart rate changes vs. changes in Ca^{2+} dynamics) and the type of agonists used. In the MI study we used isoproterenol is a more potent agonist then norepinephrine and is not cleared through neuronal reuptake and could give an exaggeration of responsiveness (Szymanski and Singh

2023). Despite these differences both models exhibited sympathetic hypo-innervation and responded to sympathetic nerve stimulation. Despite MI hearts having an elevation in ß-adrenergic sensitivity to isoproterenol and nicotine hearts having a reduced sensitivity; both models *did* respond to direct ß-adrenergic stimulation. Suggesting that despite the difference in models both MI and chronic nicotine exposure result in similar sympathetic remodeling to sympathetic nerves and ß-adrenergic stimulation.

Sympathetic Responsiveness and Chronic Nicotine Exposure

The main goal of the chronic nicotine exposure project was to elucidate the mechanisms by which chronic nicotine exposure leads to Ca^{2+} mishandling, electrophysiological changes, and potential arrhythmogenesis. In this study, we found that chronic nicotine exposure results in elevated *ex vivo* baseline heart rates, suggesting that chronic nicotine exposure may result in elevated basal sympathetic nerve activity or perhaps functional or structural changes in the sinoatrial node. We also found that nicotine hearts had higher SNS thresholds, indicating a reduced responsiveness to sympathetic nerve stimulation. Chronic nicotine exposure also results in increased susceptibility to APD and CaT alternans that does not improve with SNS and could be pro-arrhythmic. These results could be explained by sympathetic hypo-innervation of the myocardium and a reduced sensitivity to ß-adrenergic stimulation.

Significance:

The findings presented in the dissertation are extremely significant to the advancement of the cardiovascular field for a number of reasons. Firstly, the innervated rabbit heart model allows for

direct physiological sympathetic nerve stimulation in order to mechanistically study sympathetic remodeling in cardiovascular diseases (CVD) and toxin exposure that may exacerbate CVD. Additionally, most of the experimental work on sympathetic remodeling and hyperactivity post-MI has been done in rodents. Here, we present data that corroborates previous findings in a more human-like model. Lastly, with our nicotine study we determined that 28 days of nicotine exposure results in potentially detrimental sympathetic and electrophysiological remodeling that could be exacerbated in habitual tobacco and e-cigarette users. Currently, youth and young adults represent the fastest growing group of e-cigarette users and the cardiac effects of nicotine on this potentially vulnerable population is unknown. Thus, data from this study may have implications for tobacco products and other nicotine containing products.

Future Works:

Myocardial Infarction Study Future Works:

In our MI study, we focused primarily on determining the presence of CSPGs and associated hypo-innervation, and whether that is associated with electrophysiological remodeling post-MI. Currently, there are experimental therapeutics in development that target the protein tyrosine phosphatase receptor sigma (PTPσ), which is the receptor on sympathetic neurons that binds CSPGs. Pharmacological inhibition of PTPσ has been shown to promote reinnervation of the infarct post-MI in rodent models (Blake et al. 2023; 2022b). By confirming the presence of CSPGs in the post-MI rabbit heart, our data strongly support that pharmacological inhibition of PTPσ may be a promising translational therapeutic target. An obvious potential follow up study

would therefore be to see if pharmacological inhibition of PTPσ promotes reinnervation of sympathetic nerves in a rabbit model of MI, and whether reinnervation is anti-arrhythmic.

Chronic Nicotine Exposure Study Future Works:

In our nicotine study, we focused on the ventricular responses to chronic nicotine exposure and saw changes in some electrophysiological parameters, but not all. In this study, we did not see a significant increase in arrhythmia susceptibility, but it is possible that with longer exposure duration that we would see more dramatic changes in electrophysiological and Ca^{2+} handling parameters and an increased risk for detrimental arrhythmias. Nicotine is associated with changes in HRV; specifically, it has been found that chronic nicotine users have a reduced HRV which indicates an elevation in sympathetic tone (Moheimani, Bhetraratana, Yin, et al. 2017). Although we did not perform any *in vivo* work in this study, it is possible that there are changes in HRV occurring and that further experimental work could elucidate the changes in HRV seen in the human population. We did see an elevation in *ex vivo* heart rate, which could indicate potential structural or electrophysiological changes in the sinoatrial node itself. In atrial tissue slices treated with nicotine it was found that there was an increased expression of collagen III, a major constituent of atrial fibrosis (Goette et al. 2007). Additionally, a study on post-MI canine hearts found that nicotine exposure caused a significant increase in atrial fibrosis and a mild increase in canine hearts without MI (Miyauchi et al. 2005). These changes in fibrosis can interfere with conduction and create a substrate to sustain atrial arrythmias and it would be of interest to investigate the mechanisms by which nicotine contributes to the increased risk of atrial fibrillation associated with smoking (Staerk et al. 2017; Andrade et al. 2014).

References

Adabag, Selçuk, Patrick Zimmerman, Daniel Lexcen, and Alan Cheng. 2021. "Predictors of Sudden Cardiac Arrest Among Patients With Post-Myocardial Infarction Ejection Fraction Greater Than 35%." *Journal of the American Heart Association* 10 (14): e020993. https://doi.org/10.1161/JAHA.121.020993.

Aflaki, Mona, Xiao-Yan Qi, Ling Xiao, Balazs Ordog, Artavazd Tadevosyan, Xiaobin Luo, Ange Maguy, Yanfen Shi, Jean-Claude Tardif, and Stanley Nattel. 2014. "Exchange Protein Directly Activated by CAMP Mediates Slow Delayed-Rectifier Current

Remodeling by Sustained β-Adrenergic Activation in Guinea Pig Hearts." *Circulation Research* 114 (6): 993–1003. https://doi.org/10.1161/CIRCRESAHA.113.302982.

Ajijola, Olujimi A., Robert L. Lux, Anadjeet Khahera, OhJin Kwon, Eric Aliotta, Daniel B. Ennis, Michael C. Fishbein, Jeffrey L. Ardell, and Kalyanam Shivkumar. 2017. "Sympathetic Modulation of Electrical Activation in Normal and Infarcted Myocardium: Implications for Arrhythmogenesis." *American Journal of Physiology-Heart and Circulatory Physiology* 312 (3): H608–21. https://doi.org/10.1152/ajpheart.00575.2016.

Akuzawa-Tateyama, Miyuki, Michihiro Tateyama, and Rikuo Ochi. 2006. "Sustained β-Adrenergic Stimulation Increased L-Type Ca2+ Channel Expression in Cultured Quiescent Ventricular Myocytes." *The Journal of Physiological Sciences* 56 (2): 165–72. https://doi.org/10.2170/physiolsci.RP001406.

Ali, Fatma Romeh M. 2023. "E-Cigarette Unit Sales by Product and Flavor Type, and Top-Selling Brands, United States, 2020–2022." *MMWR. Morbidity and Mortality Weekly Report* 72. https://doi.org/10.15585/mmwr.mm7225a1.

Andrade, Jason, Paul Khairy, Dobromir Dobrev, and Stanley Nattel. 2014. "The Clinical Profile and Pathophysiology of Atrial Fibrillation." *Circulation Research* 114 (9): 1453–68. https://doi.org/10.1161/CIRCRESAHA.114.303211.

Aune, Dagfinn, Sabrina Schlesinger, Teresa Norat, and Elio Riboli. 2018. "Tobacco Smoking and the Risk of Sudden Cardiac Death: A Systematic Review and Meta-Analysis of Prospective Studies." *European Journal of Epidemiology* 33 (6): 509–21. https://doi.org/10.1007/s10654-017-0351-y.

Bai, Juan, Chongyu Ren, Wei Hao, Rui Wang, and Ji-Min Cao. 2008. "Chemical Sympathetic Denervation, Suppression of Myocardial Transient Outward Potassium Current, and Ventricular Fibrillation in the Rat." *Canadian Journal of Physiology and Pharmacology* 86 (10): 700–709. https://doi.org/10.1139/Y08-075.

Barua, Rajat S., and John A. Ambrose. 2013. "Mechanisms of Coronary Thrombosis in Cigarette Smoke Exposure." *Arteriosclerosis, Thrombosis, and Vascular Biology* 33 (7): 1460–67. https://doi.org/10.1161/ATVBAHA.112.300154.

Belevych, Andriy E., Dmitry Terentyev, Radmila Terentyeva, Yoshinori Nishijima, Arun Sridhar, Robert L. Hamlin, Cynthia A. Carnes, and Sandor Györke. 2011. "The Relationship between Arrhythmogenesis and Impaired Contractility in Heart Failure: Role of Altered Ryanodine Receptor Function." *Cardiovascular Research* 90 (3): 493–502. https://doi.org/10.1093/cvr/cvr025.

Bell, Robert M., Mihaela M. Mocanu, and Derek M. Yellon. 2011. "Retrograde Heart Perfusion: The Langendorff Technique of Isolated Heart Perfusion." *Journal of Molecular and Cellular Cardiology* 50 (6): 940–50. https://doi.org/10.1016/j.yjmcc.2011.02.018.

Benowitz, Neal L., and Andrea D. Burbank. 2016. "Cardiovascular Toxicity of Nicotine: Implications for Electronic Cigarette Use." *Trends in Cardiovascular Medicine* 26 (6): 515–23. https://doi.org/10.1016/j.tcm.2016.03.001.

Benowitz, Neal L., and Joseph B. Fraiman. 2017. "Cardiovascular Effects of Electronic Cigarettes." *Nature Reviews. Cardiology* 14 (8): 447–56. https://doi.org/10.1038/nrcardio.2017.36.

Bers, Donald M. 2002a. "Cardiac Excitation–Contraction Coupling." *Nature* 415 (6868): 198–205. https://doi.org/10.1038/415198a.

———. 2002b. "Cardiac Excitation–Contraction Coupling." *Nature* 415 (6868): 198–205. https://doi.org/10.1038/415198a.

Beuckelmann, D J, M Näbauer, and E Erdmann. 1993. "Alterations of K+ Currents in Isolated Human Ventricular Myocytes from Patients with Terminal Heart Failure." *Circulation Research* 73 (2): 379–85. https://doi.org/10.1161/01.RES.73.2.379.

Blackwell, Daniel J., Jeffrey Schmeckpeper, and Bjorn C. Knollmann. 2022. "Animal Models to Study Cardiac Arrhythmias." *Circulation Research* 130 (12): 1926–64. https://doi.org/10.1161/CIRCRESAHA.122.320258.

Blake, Matthew R., Diana C. Parrish, Melanie A. Staffenson, Morgan A. Johnson, William R. Woodward, and Beth A. Habecker. 2023. "Loss of Chondroitin Sulfate Proteoglycan Sulfation Allows Delayed Sympathetic Reinnervation after Cardiac Ischemia–Reperfusion." *Physiological Reports* 11 (10): e15702. https://doi.org/10.14814/phy2.15702.

Blake, Matthew R, Diana C Parrish, Melanie A Staffenson, Shanice Sueda, William R Woodward, and Beth A Habecker. 2022a. "Chondroitin Sulfate Proteoglycan 4,6 Sulfation Regulates Sympathetic Nerve Regeneration after Myocardial Infarction." Edited by Kalyanam Shivkumar, Mone Zaidi, Kalyanam Shivkumar, Hanjun Wang, and Pradeep S Rajendran. *ELife* 11 (May): e78387. https://doi.org/10.7554/eLife.78387.

———. 2022b. "Chondroitin Sulfate Proteoglycan 4,6 Sulfation Regulates Sympathetic Nerve Regeneration after Myocardial Infarction." Edited by Kalyanam Shivkumar, Mone Zaidi, Kalyanam Shivkumar, Hanjun Wang, and Pradeep S Rajendran. *ELife* 11 (May): e78387. https://doi.org/10.7554/eLife.78387.

Boateng, Stephen, and Timothy Sanborn. 2013. “Acute Myocardial Infarction.” *Disease-a-Month*, Approach to Clinical Cardiac Emergencies, 59 (3): 83–96. https://doi.org/10.1016/j.disamonth.2012.12.004.

Boogers, Mark J., C. Jan Willem Borleffs, Maureen M. Henneman, Bommel Rutger J. van, Ramshorst Jan van, Eric Boersma, -Schneider Petra Dibbets, et al. 2010. “Cardiac Sympathetic Denervation Assessed With 123-Iodine Metaiodobenzylguanidine Imaging Predicts Ventricular Arrhythmias in Implantable Cardioverter-Defibrillator Patients.” *Journal of the American College of Cardiology* 55 (24): 2769–77. https://doi.org/10.1016/j.jacc.2009.12.066.

Borlaug, Barry A., and Walter J. Paulus. 2011. “Heart Failure with Preserved Ejection Fraction: Pathophysiology, Diagnosis, and Treatment.” *European Heart Journal* 32 (6): 670–79. https://doi.org/10.1093/eurheartj/ehq426.

Bristow, M R, R Ginsburg, V Umans, M Fowler, W Minobe, R Rasmussen, P Zera, R Menlove, P Shah, and S Jamieson. 1986. “ß 1- and ß 2-Adrenergic-Receptor Subpopulations in Nonfailing and Failing Human Ventricular Myocardium: Coupling of Both Receptor Subtypes to Muscle Contraction and Selective ß 1-Receptor down-Regulation in Heart Failure.” *Circulation Research* 59 (3): 297–309. https://doi.org/10.1161/01.RES.59.3.297.

Bristow, Michael R., Robert Ginsburg, Wayne Minobe, Roger S. Cubicciotti, W. Scott Sageman, Keith Lurie, Margaret E. Billingham, Donald C. Harrison, and Edward B. Stinson. 1982. “Decreased Catecholamine Sensitivity and β-Adrenergic-Receptor Density in Failing Human Hearts.” *New England Journal of Medicine* 307 (4): 205–11. https://doi.org/10.1056/NEJM198207223070401.

Caldwell, Jessica L., I-Ju Lee, Lena Ngo, Lianguo Wang, Sherif Bahriz, Bing Xu, Donald M. Bers, et al. 2023. “Whole-Heart Multiparametric Optical Imaging Reveals Sex-Dependent Heterogeneity in CAMP Signaling and Repolarization Kinetics.” *Science Advances* 9 (3): eadd5799. https://doi.org/10.1126/sciadv.add5799.

Chatterjee, Neal A., Ravi V. Shah, Venkatesh L. Murthy, Amy Praestgaard, Sanjiv J. Shah, Corey E. Ventetuolo, R. Graham Barr, et al. 2017. “Right Ventricular Structure and Function Are Associated With Incident Atrial Fibrillation.” *Circulation: Arrhythmia and Electrophysiology* 10 (1): e004738. https://doi.org/10.1161/CIRCEP.116.004738.

Chen, Chao-Yin, Drin Chow, Nipavan Chiamvimonvat, Kathryn A. Glatter, Ning Li, Yuxia He, Kent E. Pinkerton, and Ann C. Bonham. 2008. “Short-Term Secondhand Smoke Exposure Decreases Heart Rate Variability and Increases Arrhythmia Susceptibility in Mice.” *American Journal of Physiology-Heart and Circulatory Physiology* 295 (2): H632–39. https://doi.org/10.1152/ajpheart.91535.2007.

Chen, Lan S., Shengmei Zhou, Michael C. Fishbein, and Peng-Sheng Chen. 2007. “New Perspectives on the Role of Autonomic Nervous System in the Genesis of Arrhythmias.”

Journal of Cardiovascular Electrophysiology 18 (1): 123–27. https://doi.org/10.1111/j.1540-8167.2006.00590.x.

Chou, Chung-Chuan, Shengmei Zhou, Hideki Hayashi, Motoki Nihei, Yen-Bin Liu, Ming-Shien Wen, San-Jou Yeh, et al. 2007. "Remodelling of Action Potential and Intracellular Calcium Cycling Dynamics during Subacute Myocardial Infarction Promotes Ventricular Arrhythmias in Langendorff-Perfused Rabbit Hearts." *The Journal of Physiology* 580 (3): 895–906. https://doi.org/10.1113/jphysiol.2006.120659.

Chudin, E., J. Goldhaber, A. Garfinkel, J. Weiss, and B. Kogan. 1999. "Intracellular Ca2+ Dynamics and the Stability of Ventricular Tachycardia." *Biophysical Journal* 77 (6): 2930–41. https://doi.org/10.1016/S0006-3495(99)77126-2.

Clauss, Sebastian, Christina Bleyer, Dominik Schüttler, Philipp Tomsits, Simone Renner, Nikolai Klymiuk, Reza Wakili, Steffen Massberg, Eckhard Wolf, and Stefan Kääb. 2019. "Animal Models of Arrhythmia: Classic Electrophysiology to Genetically Modified Large Animals." *Nature Reviews Cardiology* 16 (8): 457–75. https://doi.org/10.1038/s41569-019-0179-0.

Coppini, Raffaele, Cecilia Ferrantini, Lina Yao, Peidong Fan, Martina Del Lungo, Francesca Stillitano, Laura Sartiani, et al. 2013. "Late Sodium Current Inhibition Reverses Electromechanical Dysfunction in Human Hypertrophic Cardiomyopathy." *Circulation* 127 (5): 575–84. https://doi.org/10.1161/CIRCULATIONAHA.112.134932.

Cornelius, Monica E. 2023. "Tobacco Product Use Among Adults – United States, 2021." *MMWR. Morbidity and Mortality Weekly Report* 72. https://doi.org/10.15585/mmwr.mm7218a1.

Coronel, R., Ronald Wilders, Arie O. Verkerk, Rob F. Wiegerinck, David Benoist, and Olivier Bernus. 2013. "Electrophysiological Changes in Heart Failure and Their Implications for Arrhythmogenesis." *Biochimica et Biophysica Acta (BBA) - Molecular Basis of Disease* 1832 (12): 2432–41. https://doi.org/10.1016/j.bbadis.2013.04.002.

CURTIS, MICHAEL J, and MICHAEL J A WALKER. 1988. "Quantification of Arrhythmias Using Scoring Systems: An Examination of Seven Scores in an in Vivo Model of Regional Myocardial Ischaemia." *Cardiovascular Research* 22 (9): 656–65. https://doi.org/10.1093/cvr/22.9.656.

Czernin, Johannes, and Christian Waldherr. 2003. "Cigarette Smoking and Coronary Blood Flow." *Progress in Cardiovascular Diseases*, Issues on Smoking and Cardiovascular Disease, Part I, 45 (5): 395–404. https://doi.org/10.1053/pcad.2003.00104.

Dale, H. H., and P. P. Laidlaw. 1912. "The Significance of the Suprarenal Capsules in the Action of Certain Alkaloids." *The Journal of Physiology* 45 (1–2): 1–26. https://www.ncbi.nlm.nih.gov/pmc/articles/PMC1512877/.

De Jesus, Nicole M., Lianguo Wang, Johnny Lai, Robert R. Rigor, Samantha D. Francis Stuart, Donald M. Bers, Merry L. Lindsey, and Crystal M. Ripplinger. 2017. "Antiarrhythmic Effects of Interleukin 1 Inhibition after Myocardial Infarction." *Heart Rhythm* 14 (5): 727–36. https://doi.org/10.1016/j.hrthm.2017.01.027.

Deo, Rajat, Faye L. Norby, Ronit Katz, Nona Sotoodehnia, Selcuk Adabag, Christopher R. DeFilippi, Bryan Kestenbaum, et al. 2016. "Development and Validation of a Sudden Cardiac Death Prediction Model for the General Population." *Circulation* 134 (11): 806–16. https://doi.org/10.1161/CIRCULATIONAHA.116.023042.

DeSantiago, Jaime, Xun Ai, Mohammed Islam, Georgia Acuna, Mark T. Ziolo, Donald M. Bers, and Steven M. Pogwizd. 2008. "Arrhythmogenic Effects of B2-Adrenergic Stimulation in the Failing Heart Are Attributable to Enhanced Sarcoplasmic Reticulum Ca Load." *Circulation Research* 102 (11): 1389–97. https://doi.org/10.1161/CIRCRESAHA.107.169011.

DiFrancesco, Dario. 2010. "The Role of the Funny Current in Pacemaker Activity." *Circulation Research* 106 (3): 434–46. https://doi.org/10.1161/CIRCRESAHA.109.208041.

DiFrancesco, Dario, and Paolo Tortora. 1991. "Direct Activation of Cardiac Pacemaker Channels by Intracellular Cyclic AMP." *Nature* 351 (6322): 145–47. https://doi.org/10.1038/351145a0.

Dvorakova, Magdalena, Katrin S. Lips, Dörthe Brüggmann, Jana Slavikova, Jitka Kuncova, and Wolfgang Kummer. 2005. "Developmental Changes in the Expression of Nicotinic Acetylcholine Receptor α-Subunits in the Rat Heart." *Cell and Tissue Research* 319 (2): 201–9. https://doi.org/10.1007/s00441-004-1008-1.

Ellermann, Christian, Julian Wolfes, Lars Eckardt, and Gerrit Frommeyer. 2021. "Role of the Rabbit Whole-Heart Model for Electrophysiologic Safety Pharmacology of Non-Cardiovascular Drugs." *EP Europace* 23 (6): 828–36. https://doi.org/10.1093/europace/euaa288.

Fallavollita, James A., Jonathan D. Dare, Randolph L. Carter, Sunil Baldwa, and John M. Canty. 2017. "Denervated Myocardium Is Preferentially Associated With Sudden Cardiac Arrest in Ischemic Cardiomyopathy." *Circulation: Cardiovascular Imaging* 10 (8): e006446. https://doi.org/10.1161/CIRCIMAGING.117.006446.

Fallavollita, James A., Brendan M. Heavey, Andrew J. Luisi, Suzanne M. Michalek, Sunil Baldwa, Terry L. Mashtare, Alan D. Hutson, et al. 2014. "Regional Myocardial Sympathetic Denervation Predicts the Risk of Sudden Cardiac Arrest in Ischemic Cardiomyopathy." *Journal of the American College of Cardiology* 63 (2): 141–49. https://doi.org/10.1016/j.jacc.2013.07.096.

Fleischmann, Bernd K., Yaqi Duan, Yun Fan, Torsten Schoneberg, Andreas Ehlich, Nibedita Lenka, Serge Viatchenko-Karpinski, Lutz Pott, Juergen Hescheler, and Bernd Fakler.

2004. “Differential Subunit Composition of the G Protein–Activated Inward-Rectifier Potassium Channel during Cardiac Development.” *The Journal of Clinical Investigation* 114 (7): 994–1001. https://doi.org/10.1172/JCI15925.

Flint, Alexander C., Carol Conell, Xiushui Ren, Nader M. Banki, Sheila L. Chan, Vivek A. Rao, Ronald B. Melles, and Deepak L. Bhatt. 2019. “Effect of Systolic and Diastolic Blood Pressure on Cardiovascular Outcomes.” *The New England Journal of Medicine* 381 (3): 243–51. https://doi.org/10.1056/NEJMoa1803180.

Francis Stuart, Samantha D., Lianguo Wang, William R. Woodard, G. Andre Ng, Beth A. Habecker, and Crystal M. Ripplinger. 2018. “Age-Related Changes in Cardiac Electrophysiology and Calcium Handling in Response to Sympathetic Nerve Stimulation.” *The Journal of Physiology* 596 (17): 3977–91. https://doi.org/10.1113/JP276396.

Fu, Ying, Xinyan Huang, Huailing Zhong, Richard M. Mortensen, Louis G. D’Alecy, and Richard R. Neubig. 2006. “Endogenous RGS Proteins and Gα Subtypes Differentially Control Muscarinic and Adenosine-Mediated Chronotropic Effects.” *Circulation Research* 98 (5): 659–66. https://doi.org/10.1161/01.RES.0000207497.50477.60.

Gallucci, Giuseppina, Alfredo Tartarone, Rosa Lerose, Anna Vittoria Lalinga, and Alba Maria Capobianco. 2020. “Cardiovascular Risk of Smoking and Benefits of Smoking Cessation.” *Journal of Thoracic Disease* 12 (7): 3866–76. https://doi.org/10.21037/jtd.2020.02.47.

Gardner, R. T., L. Wang, B. T. Lang, J. M. Cregg, C. L. Dunbar, W. R. Woodward, J. Silver, C. M. Ripplinger, and B. A. Habecker. 2015. “Targeting Protein Tyrosine Phosphatase σ after Myocardial Infarction Restores Cardiac Sympathetic Innervation and Prevents Arrhythmias.” *Nature Communications* 6 (1): 6235. https://doi.org/10.1038/ncomms7235.

Gardner, Ryan T., and Beth A. Habecker. 2013. “Infarct-Derived Chondroitin Sulfate Proteoglycans Prevent Sympathetic Reinnervation after Cardiac Ischemia-Reperfusion Injury.” *Journal of Neuroscience* 33 (17): 7175–83. https://doi.org/10.1523/JNEUROSCI.5866-12.2013.

Gardner, Ryan T., Crystal M. Ripplinger, Rachel C. Myles, and Beth A. Habecker. 2016. “Molecular Mechanisms of Sympathetic Remodeling and Arrhythmias.” *Circulation: Arrhythmia and Electrophysiology* 9 (2): e001359. https://doi.org/10.1161/CIRCEP.115.001359.

Gibbons, Christopher H. 2019. “Chapter 27 - Basics of Autonomic Nervous System Function.” In *Handbook of Clinical Neurology*, edited by Kerry H. Levin and Patrick Chauvel, 160:407–18. Clinical Neurophysiology: Basis and Technical Aspects. Elsevier. https://doi.org/10.1016/B978-0-444-64032-1.00027-8.

Gillespie, Mark N., Joseph O. Owasoyo, Judith A. Kiritsy-Roy, William N. O'Connor, and Glen R. Van Loon. 1985. "Exaggerated Nicotine-Induced Norepinephrine Release from Atherosclerotic Rabbit Hearts." *Toxicology* 37 (1): 147–57. https://doi.org/10.1016/0300-483X(85)90120-9.

Goette, Andreas, Uwe Lendeckel, Anja Kuchenbecker, Alicja Bukowska, Brigitte Peters, Helmut U. Klein, Christof Huth, and Christoph Röcken. 2007. "Cigarette Smoking Induces Atrial Fibrosis in Humans via Nicotine." *Heart* 93 (9): 1056–63. https://doi.org/10.1136/hrt.2005.087171.

Goniewicz, Maciej Lukasz, Rachel Boykan, Catherine R. Messina, Alison Eliscu, and Jonatan Tolentino. 2019. "High Exposure to Nicotine among Adolescents Who Use Juul and Other Vape Pod Systems ('Pods')." *Tobacco Control* 28 (6): 676–77. https://doi.org/10.1136/tobaccocontrol-2018-054565.

Gourlay, Steven G., and Neal L. Benowitz. 1997. "Arteriovenous Differences in Plasma Concentration of Nicotine and Catecholamines and Related Cardiovascular Effects after Smoking, Nicotine Nasal Spray, and Intravenous Nicotine." *Clinical Pharmacology & Therapeutics* 62 (4): 453–63. https://doi.org/10.1016/S0009-9236(97)90124-7.

Grilli, Massimo, Monica Parodi, Maurizio Raiteri, and Mario Marchi. 2005. "Chronic Nicotine Differentially Affects the Function of Nicotinic Receptor Subtypes Regulating Neurotransmitter Release." *Journal of Neurochemistry* 93 (5): 1353–60. https://doi.org/10.1111/j.1471-4159.2005.03126.x.

He, Hairong, Zhenyu Pan, Jiayuan Wu, Chuanyu Hu, Ling Bai, and Jun Lyu. 2022. "Health Effects of Tobacco at the Global, Regional, and National Levels: Results From the 2019 Global Burden of Disease Study." *Nicotine & Tobacco Research* 24 (6): 864–70. https://doi.org/10.1093/ntr/ntab265.

Henning, R. J., I. R. Khalil, and M. N. Levy. 1990. "Vagal Stimulation Attenuates Sympathetic Enhancement of Left Ventricular Function." *American Journal of Physiology-Heart and Circulatory Physiology* 258 (5): H1470–75. https://doi.org/10.1152/ajpheart.1990.258.5.H1470.

Jacob, Peyton, Lisa Yu, Minjiang Duan, Lita Ramos, Olivia Yturralde, and Neal L. Benowitz. 2011. "Determination of the Nicotine Metabolites Cotinine and Trans-3′-Hydroxycotinine in Biologic Fluids of Smokers and Non-Smokers Using Liquid Chromatography–Tandem Mass Spectrometry: Biomarkers for Tobacco Smoke Exposure and for Phenotyping Cytochrome P450 2A6 Activity." *Journal of Chromatography B* 879 (3): 267–76. https://doi.org/10.1016/j.jchromb.2010.12.012.

Jamali, Hina K., Fahad Waqar, and Myron C. Gerson. 2017. "Cardiac Autonomic Innervation." *Journal of Nuclear Cardiology* 24 (5): 1558–70. https://doi.org/10.1007/s12350-016-0725-7.

Kääb, Stefan, H. Bradley Nuss, Nipavan Chiamvimonvat, Brian O'Rourke, Peter H. Pak, David A. Kass, Eduardo Marban, and Gordon F. Tomaselli. 1996. "Ionic Mechanism of Action Potential Prolongation in Ventricular Myocytes From Dogs With Pacing-Induced Heart Failure." *Circulation Research* 78 (2): 262–73. https://doi.org/10.1161/01.RES.78.2.262.

Kagan, Anna, Yonathan F. Melman, Andrew Krumerman, and Thomas V. McDonald. 2002. "14-3-3 Amplifies and Prolongs Adrenergic Stimulation of HERG K+ Channel Activity." *The EMBO Journal* 21 (8): 1889–98. https://doi.org/10.1093/emboj/21.8.1889.

Kang, C., J. A. Brennan, S. Kuzmiak-Glancy, K. E. Garrott, M. W. Kay, and I. R. Efimov. 2016. "Technical Advances in Studying Cardiac Electrophysiology – Role of Rabbit Models." *Progress in Biophysics and Molecular Biology*, Focussed Issue on Past, Present and Future of Non-murine (Lagomorph) Model Systems as Experimental and Computational Drivers of Progress in Cardiac Biophysics, 121 (2): 97–109. https://doi.org/10.1016/j.pbiomolbio.2016.05.006.

Kawano, H., Ryozo Okada, and Katsusuke Yano. 2003. "Histological Study on the Distribution of Autonomic Nerves in the Human Heart." *Heart and Vessels* 18 (1): 32–39. https://doi.org/10.1007/s003800300005.

Kazbanov, Ivan V., Kirsten H. W. J. ten Tusscher, and Alexander V. Panfilov. 2016. "Effects of Heterogeneous Diffuse Fibrosis on Arrhythmia Dynamics and Mechanism." *Scientific Reports* 6 (1): 20835. https://doi.org/10.1038/srep20835.

Kemp, Clinton D., and John V. Conte. 2012. "The Pathophysiology of Heart Failure." *Cardiovascular Pathology* 21 (5): 365–71. https://doi.org/10.1016/j.carpath.2011.11.007.

Kim, Hyun-Ji, and Ho-Sang Shin. 2013. "Determination of Tobacco-Specific Nitrosamines in Replacement Liquids of Electronic Cigarettes by Liquid Chromatography–Tandem Mass Spectrometry." *Journal of Chromatography A* 1291 (May): 48–55. https://doi.org/10.1016/j.chroma.2013.03.035.

Kimura, Kensuke, Masaki Ieda, and Keiichi Fukuda. 2012. "Development, Maturation, and Transdifferentiation of Cardiac Sympathetic Nerves." *Circulation Research* 110 (2): 325–36. https://doi.org/10.1161/CIRCRESAHA.111.257253.

Kiuchi, K., R. P. Shannon, K. Komamura, D. J. Cohen, C. Bianchi, C. J. Homcy, S. F. Vatner, and D. E. Vatner. 1993. "Myocardial ß-Adrenergic Receptor Function during the Development of Pacing-Induced Heart Failure." *The Journal of Clinical Investigation* 91 (3): 907–14. https://doi.org/10.1172/JCI116312.

Kléber, André G., and Yoram Rudy. 2004. "Basic Mechanisms of Cardiac Impulse Propagation and Associated Arrhythmias." *Physiological Reviews* 84 (2): 431–88. https://doi.org/10.1152/physrev.00025.2003.

Laurita, Kenneth R., and David S. Rosenbaum. 2008. “Cellular Mechanisms of Arrhythmogenic Cardiac Alternans.” *Progress in Biophysics and Molecular Biology*, Life and Mechanosensitivity, 97 (2): 332–47. https://doi.org/10.1016/j.pbiomolbio.2008.02.014.

Laustiola, K E, R Lassila, J Kaprio, and M Koskenvuo. 1988. “Decreased ß-Adrenergic Receptor Density and Catecholamine Response in Male Cigarette Smokers. A Study of Monozygotic Twin Pairs Discordant for Smoking.” *Circulation* 78 (5): 1234–40. https://doi.org/10.1161/01.CIR.78.5.1234.

Lefkowitz, Robert J., Howard A. Rockman, and Walter J. Koch. 2000. “Catecholamines, Cardiac β-Adrenergic Receptors, and Heart Failure.” *Circulation* 101 (14): 1634–37. https://doi.org/10.1161/01.CIR.101.14.1634.

Leimbach, W N, B G Wallin, R G Victor, P E Aylward, G Sundlöf, and A L Mark. 1986. “Direct Evidence from Intraneural Recordings for Increased Central Sympathetic Outflow in Patients with Heart Failure.” *Circulation* 73 (5): 913–19. https://doi.org/10.1161/01.CIR.73.5.913.

Li, Danshi, Samir Fareh, Tack Ki Leung, and Stanley Nattel. 1999. “Promotion of Atrial Fibrillation by Heart Failure in Dogs.” *Circulation* 100 (1): 87–95. https://doi.org/10.1161/01.CIR.100.1.87.

Liao, Zhandi, Dean Lockhead, Eric D. Larson, and Catherine Proenza. 2010. “Phosphorylation and Modulation of Hyperpolarization-Activated HCN4 Channels by Protein Kinase A in the Mouse Sinoatrial Node.” *Journal of General Physiology* 136 (3): 247–58. https://doi.org/10.1085/jgp.201010488.

Lim, Hyun-hee, and Ho-Sang Shin. 2013. “Measurement of Aldehydes in Replacement Liquids of Electronic Cigarettes by Headspace Gas Chromatography-Mass Spectrometry.” *Bulletin of the Korean Chemical Society* 34 (September). https://doi.org/10.5012/bkcs.2013.34.9.2691.

Lindsey, Merry L., Roberto Bolli, John M. Canty, Xiao-Jun Du, Nikolaos G. Frangogiannis, Stefan Frantz, Robert G. Gourdie, et al. 2018a. “Guidelines for Experimental Models of Myocardial Ischemia and Infarction.” *American Journal of Physiology-Heart and Circulatory Physiology* 314 (4): H812–38. https://doi.org/10.1152/ajpheart.00335.2017.

———. 2018b. “Guidelines for Experimental Models of Myocardial Ischemia and Infarction.” *American Journal of Physiology-Heart and Circulatory Physiology* 314 (4): H812–38. https://doi.org/10.1152/ajpheart.00335.2017.

Lindsey, Merry L., Keith R. Brunt, Jonathan A. Kirk, Petra Kleinbongard, John W. Calvert, Lisandra E. de Castro Brás, Kristine Y. DeLeon-Pennell, et al. 2021. “Guidelines for in Vivo Mouse Models of Myocardial Infarction.” *American Journal of Physiology-Heart and Circulatory Physiology* 321 (6): H1056–73. https://doi.org/10.1152/ajpheart.00459.2021.

Lisko, Joseph G., Hang Tran, Stephen B. Stanfill, Benjamin C. Blount, and Clifford H. Watson. 2015. “Chemical Composition and Evaluation of Nicotine, Tobacco Alkaloids, PH, and Selected Flavors in E-Cigarette Cartridges and Refill Solutions.” *Nicotine & Tobacco Research* 17 (10): 1270–78. https://doi.org/10.1093/ntr/ntu279.

Löffelholz, K. 1970. “Autoinhibition of Nicotinic Release of Noradrenaline from Postganglionic Sympathetic Nerves.” *Naunyn-Schmiedebergs Archiv Für Pharmakologie* 267 (1): 49–63. https://doi.org/10.1007/BF00997114.

Lou, Qing, Ajit Janardhan, and Igor R. Efimov. 2012. “Remodeling of Calcium Handling in Human Heart Failure.” *Advances in Experimental Medicine and Biology* 740: 1145–74. https://doi.org/10.1007/978-94-007-2888-2_52.

Lymperopoulos, Anastasios, Natalie Cora, Jennifer Maning, Ava R. Brill, and Anastasiya Sizova. 2021. “Signaling and Function of Cardiac Autonomic Nervous System Receptors: Insights from the GPCR Signalling Universe.” *The FEBS Journal* 288 (8): 2645–59. https://doi.org/10.1111/febs.15771.

MacLennan, David H., and Evangelia G. Kranias. 2003. “Phospholamban: A Crucial Regulator of Cardiac Contractility.” *Nature Reviews Molecular Cell Biology* 4 (7): 566–77. https://doi.org/10.1038/nrm1151.

Madamanchi, Aasakiran. 2007. “β-Adrenergic Receptor Signaling in Cardiac Function and Heart Failure.” *McGill Journal of Medicine : MJM* 10 (2): 99–104. https://www.ncbi.nlm.nih.gov/pmc/articles/PMC2323471/.

Malliani, Alberto, Federico Lombardi, Massimo Pagani, and Sergio Cerutti. 1994. “Power Spectral Analysis of Cardiovascular Variability in Patients at Risk for Sudden Cardiac Death.” *Journal of Cardiovascular Electrophysiology* 5 (3): 274–86. https://doi.org/10.1111/j.1540-8167.1994.tb01164.x.

Marx, Steven O., Junko Kurokawa, Steven Reiken, Howard Motoike, Jeanine D’Armiento, Andrew R. Marks, and Robert S. Kass. 2002. “Requirement of a Macromolecular Signaling Complex for β Adrenergic Receptor Modulation of the KCNQ1-KCNE1 Potassium Channel.” *Science* 295 (5554): 496–99. https://doi.org/10.1126/science.1066843.

Mehta, Mahaveer C., Abnash C. Jain, Anurag Mehta, and Mike Billie. 1997. “Cardiac Arrhythmias Following Intravenous Nicotine: Experimental Study in Dogs.” *Journal of Cardiovascular Pharmacology and Therapeutics* 2 (4): 291–97. https://doi.org/10.1177/107424849700200407.

Mensah, George A., and David W. Brown. 2007. “An Overview Of Cardiovascular Disease Burden In The United States.” *Health Affairs* 26 (1): 38–48. https://doi.org/10.1377/hlthaff.26.1.38.

Mills, Edward J., Kristian Thorlund, Shawn Eapen, Ping Wu, and Judith J. Prochaska. 2014. "Cardiovascular Events Associated With Smoking Cessation Pharmacotherapies." *Circulation* 129 (1): 28–41. https://doi.org/10.1161/CIRCULATIONAHA.113.003961.

Mills, Edward J., Ping Wu, Ian Lockhart, Kumanan Wilson, and Jon O. Ebbert. 2010. "Adverse Events Associated with Nicotine Replacement Therapy (NRT) for Smoking Cessation. A Systematic Review and Meta-Analysis of One Hundred and Twenty Studies Involving 177,390 Individuals." *Tobacco Induced Diseases* 8 (1): 8. https://doi.org/10.1186/1617-9625-8-8.

Mitchell, G. A. G. 1953. "THE INNERVATION OF THE HEART." *British Heart Journal* 15 (2): 159–71. https://www.ncbi.nlm.nih.gov/pmc/articles/PMC479482/.

Miyauchi, Mizuho, Zhilin Qu, Yasushi Miyauchi, Sheng-Mei Zhou, Hui Pak, William J. Mandel, Michael C. Fishbein, Peng-Sheng Chen, and Hrayr S. Karagueuzian. 2005. "Chronic Nicotine in Hearts with Healed Ventricular Myocardial Infarction Promotes Atrial Flutter That Resembles Typical Human Atrial Flutter." *American Journal of Physiology-Heart and Circulatory Physiology* 288 (6): H2878–86. https://doi.org/10.1152/ajpheart.01165.2004.

Moheimani, Roya S., May Bhetraratana, Kacey M. Peters, Benjamin K. Yang, Fen Yin, Jeffrey Gornbein, Jesus A. Araujo, and Holly R. Middlekauff. 2017. "Sympathomimetic Effects of Acute E-Cigarette Use: Role of Nicotine and Non-Nicotine Constituents." *Journal of the American Heart Association* 6 (9): e006579. https://doi.org/10.1161/JAHA.117.006579.

Moheimani, Roya S., May Bhetraratana, Fen Yin, Kacey M. Peters, Jeffrey Gornbein, Jesus A. Araujo, and Holly R. Middlekauff. 2017. "Increased Cardiac Sympathetic Activity and Oxidative Stress in Habitual Electronic Cigarette Users: Implications for Cardiovascular Risk." *JAMA Cardiology* 2 (3): 278–84. https://doi.org/10.1001/jamacardio.2016.5303.

Murphy, Sean P., Nasrien E. Ibrahim, and James L. Januzzi Jr. 2020. "Heart Failure With Reduced Ejection Fraction: A Review." *JAMA* 324 (5): 488–504. https://doi.org/10.1001/jama.2020.10262.

Myles, Rachel C, Lianguo Wang, Donald M Bers, and Crystal M Ripplinger. 2015. "Decreased Inward Rectifying K+ Current and Increased Ryanodine Receptor Sensitivity Synergistically Contribute to Sustained Focal Arrhythmia in the Intact Rabbit Heart." *The Journal of Physiology* 593 (Pt 6): 1479–93. https://doi.org/10.1113/jphysiol.2014.279638.

Myles, Rachel C., Lianguo Wang, Chaoyi Kang, Donald M. Bers, and Crystal M. Ripplinger. 2012. "Local β-Adrenergic Stimulation Overcomes Source-Sink Mismatch to Generate Focal Arrhythmia." *Circulation Research* 110 (11): 1454–64. https://doi.org/10.1161/CIRCRESAHA.111.262345.

Ng, G. André, Kieran E. Brack, and John H. Coote. 2001a. “Effects of Direct Sympathetic and Vagus Nerve Stimulation on the Physiology of the Whole Heart – A Novel Model of Isolated Langendorff Perfused Rabbit Heart with Intact Dual Autonomic Innervation.” *Experimental Physiology* 86 (3): 319–29. https://doi.org/10.1113/eph8602146.

———. 2001b. “Effects of Direct Sympathetic and Vagus Nerve Stimulation on the Physiology of the Whole Heart – A Novel Model of Isolated Langendorff Perfused Rabbit Heart with Intact Dual Autonomic Innervation.” *Experimental Physiology* 86 (3): 319–29. https://doi.org/10.1113/eph8602146.

Ng, G.André, Stuart M Cobbe, and Godfrey L Smith. 1998. “Non-Uniform Prolongation of Intracellular Ca2+ Transients Recorded from the Epicardial Surface of Isolated Hearts from Rabbits with Heart Failure.” *Cardiovascular Research* 37 (2): 489–502. https://doi.org/10.1016/S0008-6363(97)00255-1.

Nieuwenhoven, Frans A. van, and Neil A. Turner. 2013. “The Role of Cardiac Fibroblasts in the Transition from Inflammation to Fibrosis Following Myocardial Infarction.” *Vascular Pharmacology*, Recent Advances in Cardiovascular Biology and Translational Medicine, 58 (3): 182–88. https://doi.org/10.1016/j.vph.2012.07.003.

Nishisato, Kimio, Akiyoshi Hashimoto, Tomoaki Nakata, Takahiro Doi, Hitomi Yamamoto, Daigo Nagahara, Shinya Shimoshige, Satoshi Yuda, Kazufumi Tsuchihashi, and Kazuaki Shimamoto. 2010. “Impaired Cardiac Sympathetic Innervation and Myocardial Perfusion Are Related to Lethal Arrhythmia: Quantification of Cardiac Tracers in Patients with ICDs.” *Journal of Nuclear Medicine* 51 (8): 1241–49. https://doi.org/10.2967/jnumed.110.074971.

Oakes, Joshua M., Jiaxi Xu, Tamara M. Morris, Nicholas D. Fried, Charlotte S. Pearson, Thomas D. Lobell, Nicholas W. Gilpin, Eric Lazartigues, Jason D. Gardner, and Xinping Yue. 2020. “Effects of Chronic Nicotine Inhalation on Systemic and Pulmonary Blood Pressure and Right Ventricular Remodeling in Mice.” *Hypertension* 75 (5): 1305–14. https://doi.org/10.1161/HYPERTENSIONAHA.119.14608.

Ohte, Nobuyuki, Hitomi Narita, Akihiko Iida, Hidekatsu Fukuta, Narushi Iizuka, Junichiro Hayano, Yuji Kuge, Nagara Tamaki, and Genjiro Kimura. 2012. “Cardiac β-Adrenergic Receptor Density and Myocardial Systolic Function in the Re{Citation}mote Noninfarcted Region after Prior Myocardial Infarction with Left Ventricular Remodelling.” *European Journal of Nuclear Medicine and Molecular Imaging* 39 (8): 1246–53. https://doi.org/10.1007/s00259-012-2138-4.

O’Shea, Christopher, Andrew P. Holmes, Ting Y. Yu, James Winter, Simon P. Wells, Joao Correia, Bastiaan J. Boukens, et al. 2019. “ElectroMap: High-Throughput Open-Source Software for Analysis and Mapping of Cardiac Electrophysiology.” *Scientific Reports* 9 (1): 1389. https://doi.org/10.1038/s41598-018-38263-2.

Panfilov, Alexander V. 2006. “Is Heart Size a Factor in Ventricular Fibrillation? Or How Close Are Rabbit and Human Hearts?” *Heart Rhythm* 3 (7): 862–64. https://doi.org/10.1016/j.hrthm.2005.12.022.

Pankow, James F., Kilsun Kim, Kevin J. McWhirter, Wentai Luo, Jorge O. Escobedo, Robert M. Strongin, Anna K. Duell, and David H. Peyton. 2017. “Benzene Formation in Electronic Cigarettes.” *PLOS ONE* 12 (3): e0173055. https://doi.org/10.1371/journal.pone.0173055.

Park-Lee, Eunice. 2022. “Tobacco Product Use Among Middle and High School Students — United States, 2022.” *MMWR. Morbidity and Mortality Weekly Report* 71. https://doi.org/10.15585/mmwr.mm7145a1.

Parrish, Diana C., Eric N. Alston, Hermann Rohrer, Paul Nkadi, William R. Woodward, Günther Schütz, and Beth A. Habecker. 2010. “Infarction-Induced Cytokines Cause Local Depletion of Tyrosine Hydroxylase in Cardiac Sympathetic Nerves.” *Experimental Physiology* 95 (2): 304–14. https://doi.org/10.1113/expphysiol.2009.049965.

Pellegrino, Roberto, Biagio Tinghino, Giacomo Mangiaracina, Alessandra Marani, Matteo Vitali, Carmela Protano, J Osborn, and Maria Cattaruzza. 2011. “Electronic Cigarettes: An Evaluation of Exposure to Chemicals and Fine Particulate Matter (PM).” *Annali Di Igiene : Medicina Preventiva e Di Comunità* 24 (November): 279–88.

Penela, Petronila, Javier Inserte, Paula Ramos, Antonio Rodriguez-Sinovas, David Garcia-Dorado, and Federico Mayor. 2019. “Degradation of GRK2 and AKT Is an Early and Detrimental Event in Myocardial Ischemia/Reperfusion.” *EBioMedicine* 48 (October): 605–18. https://doi.org/10.1016/j.ebiom.2019.09.019.

Pilowsky, Paul M., and Ann K. Goodchild. 2002. “Baroreceptor Reflex Pathways and Neurotransmitters: 10 Years On.” *Journal of Hypertension* 20 (9): 1675. https://journals.lww.com/jhypertension/Fulltext/2002/09000/Baroreceptor_reflex_pathways_and.00002.aspx?casa_token=72sGSPsevBQAAAAA:gucgnmVxyE4f4zzqsg6ysYa1a4aSdE_g3_R8umhv-SsKr7_k0N43bujjRYbtXi01Yo_tSqreI_nhQTNqda67MckTfA.

Pogwizd, Steven M., and Donald M. Bers. 2008. “Rabbit Models of Heart Disease.” *Drug Discovery Today: Disease Models*, Cardiovascular disease models, 5 (3): 185–93. https://doi.org/10.1016/j.ddmod.2009.02.001.

Pogwizd, Steven M., Klaus Schlotthauer, Li Li, Weilong Yuan, and Donald M. Bers. 2001. “Arrhythmogenesis and Contractile Dysfunction in Heart Failure.” *Circulation Research* 88 (11): 1159–67. https://doi.org/10.1161/hh1101.091193.

Raake, Philip W., Xiaoying Zhang, Leif E. Vinge, Henriette Brinks, Erhe Gao, Naser Jaleel, Yingxin Li, et al. 2012. “Cardiac G-Protein–Coupled Receptor Kinase 2 Ablation Induces a Novel Ca2+ Handling Phenotype Resistant to Adverse Alterations and Remodeling After Myocardial Infarction.” *Circulation* 125 (17): 2108–18. https://doi.org/10.1161/CIRCULATIONAHA.111.044255.

Ripplinger, Crystal M., Alexey V. Glukhov, Matthew W. Kay, Bastiaan J. Boukens, Nipavan Chiamvimonvat, Brian P. Delisle, Larissa Fabritz, et al. 2022. "Guidelines for Assessment of Cardiac Electrophysiology and Arrhythmias in Small Animals." *American Journal of Physiology-Heart and Circulatory Physiology* 323 (6): H1137–66. https://doi.org/10.1152/ajpheart.00439.2022.

Roger, Véronique L. 2021. "Epidemiology of Heart Failure." *Circulation Research* 128 (10): 1421–34. https://doi.org/10.1161/CIRCRESAHA.121.318172.

Santulli, Gaetano, Alfonso Campanile, Letizia Spinelli, Emiliano Assante di Panzillo, Michele Ciccarelli, Bruno Trimarco, and Guido Iaccarino. 2011. "G Protein-Coupled Receptor Kinase 2 in Patients With Acute Myocardial Infarction." *The American Journal of Cardiology* 107 (8): 1125–30. https://doi.org/10.1016/j.amjcard.2010.12.006.

Saternos, Hannah C., Daniyah A. Almarghalani, Hayley M. Gibson, Mahmood A. Meqdad, Raymond B. Antypas, Ajay Lingireddy, and Wissam A. AbouAlaiwi. 2018. "Distribution and Function of the Muscarinic Receptor Subtypes in the Cardiovascular System." *Physiological Genomics* 50 (1): 1–9. https://doi.org/10.1152/physiolgenomics.00062.2017.

Satoh, Hiroyasu. 1997. "Effects of Nicotine on Spontaneous Activity and Underlying Ionic Currents in Rabbit Sinoatrial Nodal Cells." *General Pharmacology: The Vascular System* 28 (1): 39–44. https://doi.org/10.1016/S0306-3623(96)00168-1.

Schrör, Karsten, Katja C Zimmermann, and Roman Tannhäuser. 1998. "Augmented Myocardial Ischaemia by Nicotine – Mechanisms and Their Possible Significance." *British Journal of Pharmacology* 125 (1): 79–86. https://doi.org/10.1038/sj.bjp.0702061.

Shan, Hongli, Yong Zhang, Yanjie Lu, Ying Zhang, Zhenwei Pan, Benzhi Cai, Ning Wang, et al. 2009. "Downregulation of MiR-133 and MiR-590 Contributes to Nicotine-Induced Atrial Remodelling in Canines." *Cardiovascular Research* 83 (3): 465–72. https://doi.org/10.1093/cvr/cvp130.

Shekha, Karthik, Joydeep Ghosh, Deepak Thekkoott, and Yisachar Greenberg. 2005. "Risk Stratification for Sudden Cardiac Death In Patients With Non-Ischemic Dilated Cardiomyopathy." *Indian Pacing and Electrophysiology Journal* 5 (2): 122–38. https://www.ncbi.nlm.nih.gov/pmc/articles/PMC1502083/.

Staerk, Laila, Jason A. Sherer, Darae Ko, Emelia J. Benjamin, and Robert H. Helm. 2017. "Atrial Fibrillation." *Circulation Research* 120 (9): 1501–17. https://doi.org/10.1161/CIRCRESAHA.117.309732.

Sved, A. F. 2009. "Blood Pressure: Baroreceptors." In *Encyclopedia of Neuroscience*, edited by Larry R. Squire, 259–64. Oxford: Academic Press. https://doi.org/10.1016/B978-008045046-9.00468-X.

Szymanski, Michael W., and Davinder P. Singh. 2023. “Isoproterenol.” In *StatPearls*. Treasure Island (FL): StatPearls Publishing. http://www.ncbi.nlm.nih.gov/books/NBK526042/.

Tapa, Srinivas, Lianguo Wang, Samantha D. Francis Stuart, Zhen Wang, Yanyan Jiang, Beth A. Habecker, and Crystal M. Ripplinger. 2020. “Adrenergic Supersensitivity and Impaired Neural Control of Cardiac Electrophysiology Following Regional Cardiac Sympathetic Nerve Loss.” *Scientific Reports* 10 (1): 18801. https://doi.org/10.1038/s41598-020-75903-y.

Tomaselli, Gordon F., and Douglas P. Zipes. 2004. “What Causes Sudden Death in Heart Failure?” *Circulation Research* 95 (8): 754–63. https://doi.org/10.1161/01.RES.0000145047.14691.db.

Tomek, Jakub, Blanca Rodriguez, Gil Bub, and Jordi Heijman. 2017. “β-Adrenergic Receptor Stimulation Inhibits Proarrhythmic Alternans in Postinfarction Border Zone Cardiomyocytes: A Computational Analysis.” *American Journal of Physiology - Heart and Circulatory Physiology* 313 (2): H338–53. https://doi.org/10.1152/ajpheart.00094.2017.

Ton, Anh Tuan, Michael Biet, Jean-Francois Delabre, Nathalie Morin, and Robert Dumaine. 2017. “In-Utero Exposure to Nicotine Alters the Development of the Rabbit Cardiac Conduction System and Provides a Potential Mechanism for Sudden Infant Death Syndrome.” *Archives of Toxicology* 91 (12): 3947–60. https://doi.org/10.1007/s00204-017-2006-x.

Ungerer, M, M Böhm, J S Elce, E Erdmann, and M J Lohse. 1993. “Altered Expression of ß-Adrenergic Receptor Kinase and ß 1-Adrenergic Receptors in the Failing Human Heart.” *Circulation* 87 (2): 454–63. https://doi.org/10.1161/01.CIR.87.2.454.

Valdivia, Carmen R., William W. Chu, Jielin Pu, Jason D. Foell, Robert A. Haworth, Mathew R. Wolff, Timothy J. Kamp, and Jonathan C. Makielski. 2005. “Increased Late Sodium Current in Myocytes from a Canine Heart Failure Model and from Failing Human Heart.” *Journal of Molecular and Cellular Cardiology* 38 (3): 475–83. https://doi.org/10.1016/j.yjmcc.2004.12.012.

Vaseghi, Marmar, Robert L. Lux, Aman Mahajan, and Kalyanam Shivkumar. 2012a. “Sympathetic Stimulation Increases Dispersion of Repolarization in Humans with Myocardial Infarction.” *American Journal of Physiology-Heart and Circulatory Physiology* 302 (9): H1838–46. https://doi.org/10.1152/ajpheart.01106.2011.

———. 2012b. “Sympathetic Stimulation Increases Dispersion of Repolarization in Humans with Myocardial Infarction.” *American Journal of Physiology-Heart and Circulatory Physiology* 302 (9): H1838–46. https://doi.org/10.1152/ajpheart.01106.2011.

Vermeulen, J. T., M. A. McGuire, T. Opthof, R. Coronel, J. M. de Bakker, C. Klöpping, and M. J. Janse. 1994. “Triggered Activity and Automaticity in Ventricular Trabeculae of Failing

Human and Rabbit Hearts." *Cardiovascular Research* 28 (10): 1547–54. https://doi.org/10.1093/cvr/28.10.1547.

Wang, Huizhen, Hong Shi, Liming Zhang, Marc Pourrier, Baofeng Yang, Stanley Nattel, and Zhiguo Wang. 2000. "Nicotine Is a Potent Blocker of the Cardiac A-Type K+ Channels." *Circulation* 102 (10): 1165–71. https://doi.org/10.1161/01.CIR.102.10.1165.

Wang, Huizhen, Baofeng Yang, Limin Zhang, Donghui Xu, and Zhiguo Wang. 2000. "Direct Block of Inward Rectifier Potassium Channels by Nicotine." *Toxicology and Applied Pharmacology* 164 (1): 97–101. https://doi.org/10.1006/taap.2000.8896.

Wang, Lianguo, Stefano Morotti, Srinivas Tapa, Samantha D. Francis Stuart, Yanyan Jiang, Zhen Wang, Rachel C. Myles, et al. 2019. "Different Paths, Same Destination: Divergent Action Potential Responses Produce Conserved Cardiac Fight-or-Flight Response in Mouse and Rabbit Hearts." *The Journal of Physiology* 597 (15): 3867–83. https://doi.org/10.1113/JP278016.

Wang, Lianguo, Rachel C. Myles, Nicole M. De Jesus, Alex K.P. Ohlendorf, Donald M. Bers, and Crystal M. Ripplinger. 2014. "Optical Mapping of Sarcoplasmic Reticulum Ca2+ in the Intact Heart: Ryanodine Receptor Refractoriness During Alternans and Fibrillation." *Circulation Research* 114 (9): 1410–21. https://doi.org/10.1161/CIRCRESAHA.114.302505.

Wang, Lianguo, Rachel C. Myles, I.-Ju Lee, Donald M. Bers, and Crystal M. Ripplinger. 2021. "Role of Reduced Sarco-Endoplasmic Reticulum Ca2+-ATPase Function on Sarcoplasmic Reticulum Ca2+ Alternans in the Intact Rabbit Heart." *Frontiers in Physiology* 12: 656516. https://doi.org/10.3389/fphys.2021.656516.

Wang, Lianguo, Antoinette Olivas, Samantha D. Francis Stuart, Srinivas Tapa, Matthew R. Blake, William R. Woodward, Beth A. Habecker, and Crystal M. Ripplinger. 2020. "Cardiac Sympathetic Nerve Transdifferentiation Reduces Action Potential Heterogeneity after Myocardial Infarction." *American Journal of Physiology-Heart and Circulatory Physiology* 318 (3): H558–65. https://doi.org/10.1152/ajpheart.00412.2019.

Wang, Lianguo, and Crystal M Ripplinger. 2019. "Putting the Pieces Together Using in Vivo Optical Mapping." *Cardiovascular Research* 115 (11): 1574–75. https://doi.org/10.1093/cvr/cvz089.

Wang, Zhen, Lianguo Wang, Srinivas Tapa, Kent E. Pinkerton, Chao-Yin Chen, and Crystal M. Ripplinger. 2018. "Exposure to Secondhand Smoke and Arrhythmogenic Cardiac Alternans in a Mouse Model." *Environmental Health Perspectives* 126 (12): 127001. https://doi.org/10.1289/EHP3664.

Watts, Daniel T. 1960. "The Effect of Nicotine and Smoking on the Secretion of Epinephrine*." *Annals of the New York Academy of Sciences* 90 (1): 74–80. https://doi.org/10.1111/j.1749-6632.1960.tb32619.x.

Weir, Robin A. P., John J. V. McMurray, and Eric J. Velazquez. 2006. "Epidemiology of Heart Failure and Left Ventricular Systolic Dysfunction after Acute Myocardial Infarction: Prevalence, Clinical Characteristics, and Prognostic Importance." *The American Journal of Cardiology*, Heart Failure Complicating Acute Myocardial Infarction and the Role of Aldosterone Blockade: New Insights into Epidemiology, Pathophysiology, and Effective Treatment Strategies, 97 (10, Supplement 1): 13–25. https://doi.org/10.1016/j.amjcard.2006.03.005.

Wennmalm, A. 1977. "Nicotine Stimulates Prostaglandin Formation in the Rabbit Heart." *British Journal of Pharmacology* 59 (1): 95–100. https://www.ncbi.nlm.nih.gov/pmc/articles/PMC1667691/.

Westfall, Thomas C. 1970. "Influence of Chronic Nicotine Administration on Blood Pressure and Heart Norepinephrine Turnover." *European Journal of Pharmacology* 10 (1): 19–24. https://doi.org/10.1016/0014-2999(70)90152-4.

Yashima, Masaaki, Toshihiko Ohara, Ji-Min Cao, Young-Hoon Kim, Michael C. Fishbein, William J. Mandel, Peng-Sheng Chen, and Hrayr S. Karagueuzian. 2000. "Nicotine Increases Ventricular Vulnerability to Fibrillation in Hearts with Healed Myocardial Infarction." *American Journal of Physiology-Heart and Circulatory Physiology* 278 (6): H2124–33. https://doi.org/10.1152/ajpheart.2000.278.6.H2124.

Yatani, A., Y. -T. Shen, L. Yan, W. Chen, S. -J. Kim, K. Sano, K. Irie, S. F. Vatner, and D. E. Vatner. 2006. "Down Regulation of the L-Type Ca2+ Channel, GRK2, and Phosphorylated Phospholamban: Protective Mechanisms for the Denervated Failing Heart." *Journal of Molecular and Cellular Cardiology* 40 (5): 619–28. https://doi.org/10.1016/j.yjmcc.2006.02.002.

Yokotani, Kunihiko, Shoshiro Okada, and Kumiko Nakamura. 2002. "Characterization of Functional Nicotinic Acetylcholine Receptors Involved in Catecholamine Release from the Isolated Rat Adrenal Gland." *European Journal of Pharmacology* 446 (1): 83–87. https://doi.org/10.1016/S0014-2999(02)01819-8.

Zaragoza, Carlos, Carmen Gomez-Guerrero, Jose Luis Martin-Ventura, Luis Blanco-Colio, Begoña Lavin, Beñat Mallavia, Carlos Tarin, Sebastian Mas, Alberto Ortiz, and Jesus Egido. 2011. "Animal Models of Cardiovascular Diseases." *BioMed Research International* 2011 (February): e497841. https://doi.org/10.1155/2011/497841.

Zhou, Shengmei, Lan S. Chen, Yasushi Miyauchi, Mizuho Miyauchi, Saibal Kar, Simon Kangavari, Michael C. Fishbein, Behrooz Sharifi, and Peng-Sheng Chen. 2004. "Mechanisms of Cardiac Nerve Sprouting After Myocardial Infarction in Dogs." *Circulation Research* 95 (1): 76–83. https://doi.org/10.1161/01.RES.0000133678.22968.e3.